Viscosity of CO_2-rich mixtures from 243 K to 423 K at pressures up to 155 MPa: new experimental viscosity data and modelling

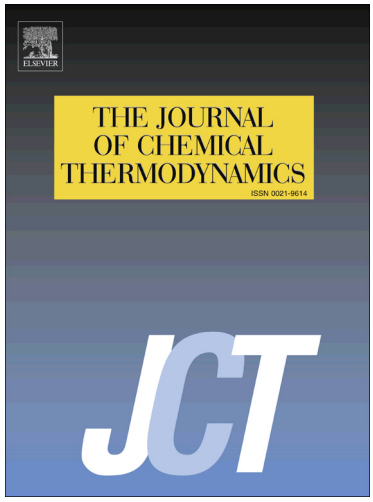

Viscosity of CO_2-rich mixtures from 243 K to 423 K at pressures up to 155 MPa: new experimental viscosity data and modelling

Mahmoud Nazeri, Antonin Chapoy, Rod Burgass, Bahman Tohidi

PII: S0021-9614(17)30397-X
DOI: https://doi.org/10.1016/j.jct.2017.11.005
Reference: YJCHT 5256

To appear in: *J. Chem. Thermodynamics*

Received Date: 31 May 2017
Revised Date: 16 October 2017
Accepted Date: 11 November 2017

Please cite this article as: M. Nazeri, A. Chapoy, R. Burgass, B. Tohidi, Viscosity of CO_2-rich mixtures from 243 K to 423 K at pressures up to 155 MPa: new experimental viscosity data and modelling, *J. Chem. Thermodynamics* (2017), doi: https://doi.org/10.1016/j.jct.2017.11.005

Viscosity of CO_2-rich mixtures from 243 K to 423 K at pressures up to 155 MPa: new experimental viscosity data and modelling

Mahmoud Nazeri[a*], Antonin Chapoy[a*], Rod Burgass[a], Bahman Tohidi[a]

Hydrates, Flow Assurance & Phase Equilibria Research Group, Institute of Petroleum Engineering, Heriot-Watt University, Edinburgh, EH14 4AS, UK

** Corresponding Authors: Mahmoud Nazeri (M.Nazeri@hw.ac.uk)*

Antonin Chapoy (Antonin.chapoy@pet.hw.ac.uk)

ABSTRACT

The viscosities of three multi-component CO_2-rich mixtures were measured using the classical capillary tube technique. The tests were conducted at pressures from 1 to 155 MPa at various temperatures from 243 to 423 K in the gas, liquid and supercritical regions. Correlative and predictive models were evaluated using the measured experimental viscosity data. The correlative model, i.e., Lohrenz-Bray-Clark (LBC) model, was tuned to match the experimental data (CO_2-LBC after tuning) and predictive models were modified by replacing the reference fluids. The predictive models in this work are based on the corresponding states (CS) theory models. The one reference fluid corresponding states model is the model originally developed by Pedersen which was modified by changing the reference fluid from methane to CO_2 (called hereafter to CO_2-Pedersen); two reference fluid corresponding states model is the Aasberg-Petersen (CS2) approach which was modified by selecting CO_2 as reference fluid for CO_2-rich fluids instead of n-decane which is suitable for hydrocarbons (CO_2-CS2 model). The SUPERTRAPP predictive model, based on the extended corresponding states (ECS) theory, was also modified by changing the reference fluid propane to carbon dioxide (CO_2-SUPERTRAPP). Comparisons for the investigated mixtures show that the overall Absolute Average Deviation (AAD) for the CO_2-Pedersen, CO_2-SUPERTRAPP, CO_2-CS2 and CO_2-LBC are 3.8%, 4.6%, 5.3% and 9.2%, respectively. Overall, the CO_2-Pedesen viscosity model is the most accurate model when predicting the viscosity of the investigated CO_2-rich mixtures. As the viscosity is a function of density, the effect of the mixture density on the mixture viscosity was investigated. Also, the viscosity reduction of pure CO_2 due to the presence of impurities in each system was demonstrated.

Keywords: *Viscosity, Carbon capture and storage (CCS), CO_2 Transport properties, CO_2 pipelines, corresponding states theory, dense liquid / supercritical CO_2*

1. Introduction

CO_2-rich pipelines are a key part of any carbon capture and storage (CCS) project. Existing CO_2 pipelines commonly contain 85-98% CO_2 with other impurities like methane, hydrogen sulphide, nitrogen, hydrogen, argon and ethane$^+$ light hydrocarbons depending on the capture technology employed for CO_2 removal [1]. Modelling phase behaviour, pressure drop, heat transfer and flow assurance in these pipelines is challenging due to the lack of thermophysical properties for CO_2 in presence of impurities as the CO_2 captured from power plants always contains impurities [2][3][4]. As transport properties have a major effect on the sizing of the equipment while the thermodynamic properties determine the feasibility of a given process, therefore, it is crucial to investigate the impact of different impurities on the thermophysical properties of CO_2-rich systems [5][6]. Therefore, accurate experimental data on the transport properties of CO_2-rich systems are required to develop accurate predictive and correlative models in order to precisely design carbon capture, transport and storage processes [7]. Consequently, models with precise predictions can lead to in CAPEX by cost-effective design and sizing of the equipment [8][9].

Another importance of the thermophysical properties in CCS is their effects on flow measurements [10]. The European Union Emission Trading Scheme (EU ETS) has an important plan to control the greenhouse gas emissions [11]. Regarding the safety concerns for leakage from the storage sites, measurement and monitoring would be a key element in CCS projects [12][13]. The EU ETS regulations require an uncertainty of ±1.5% by mass on the quantity of stored CO_2 [14]. This requires an accurate measuring of the CO_2 flow containing impurities [15]. Unlike other fluids transported in pipelines (e.g. natural gas, water and oil), the CO_2 critical point is in the vicinity of the ambient temperature and expected pressure range of CO_2 pipelines. In other words, small gradients in pressure or temperature can be resulted in a significant change on thermophysical properties of the fluid such as density, viscosity, compressibility and phase [16]. This can challenge achieving the ±1.5% uncertainty target. Also, there is a risk of phase change due to the pressure and temperature gradients and multiphase flow can arise in the pipeline which can influence both thermophysical properties and flow measurement [17][18].

Estimation of transport properties is of crucial interest to understand and estimate flow and heat transfer behaviour of fluids [19]. Viscosity is a key transport property for pipeline systems as well as sub-surface and process systems [20]. There are some methods to predict the viscosity of fluids. A widely used method to calculate the transport properties of fluids, particularly viscosity, is based on the predictions by using the corresponding states (CS) and extended corresponding states (ECS) concepts [21]. The principle of corresponding states arises from the fact that properties of many fluids are functions of critical temperature and critical density. Extended corresponding states models modify the properties by employing extra shape factors, which are functions of reduced temperature, reduced density and the acentric factor of the mixture, to account for deviations from the corresponding state principle and consequently to improve predictions [21]. Another common concept to determine the viscosity of fluids is the residual viscosity concept which is based on the observation that the difference between the dense phase viscosity and the dilute gas viscosity is a function of the mixture density and approximately independent of temperature [22] Viscosity data for binary systems of carbon dioxide and other gases can be found in the open literature over different temperature ranges and CO_2 fractions; however most of the measurements were conducted at atmospheric pressure and in the gas phase. Furthermore, in the gas phase few data were reported at pressures higher than 2.53 MPa. Table 1 summarises the available experimental viscosity data of mixtures containing CO_2 in the literature. The ranges of temperature and pressure, CO_2 fraction, state of the fluid and uncertainty are listed in the table. As can be seen, most of the available viscosity data are in the gas phase and at atmospheric pressure.

The densities of three multi-component high CO_2 content mixtures were published by authors recently [23]. In this work, new experimental viscosity data were presented for these CO_2-rich multi component mixtures. The new viscosity data are in the gas, liquid and supercritical regions from 243 K to 423 K and at pressures up to 155 MPa. In the modelling part, the correlative LBC [24] model was tuned to match to the new experimental data of CO_2-rich fluids, called CO_2-LBC. The predictive models based on corresponding states theory were also modified for the CO_2 streams with impurities. The model suggested by Fenghour et al. [25] to predict the viscosity of pure CO_2 was replaced as a reference fluid to the methane, propane and n-decane in the Pedersen [26], SUPERTRAPP [27] and Aasberg-Petersen [28] models, respectively. The modified models were called CO_2-Pedersen [29], CO_2-SUPERTRAPP and CO_2-CS2. The modified models were then evaluated using the measured viscosity data in this work.

2. Experimental

2.1. *Material*

The pure CO_2 used is this work was supplied by Air Products in research grade (N4.5) with the total impurities of less than 50 part per million in volume (ppm_v) (see Table 2). The mixture materials include three multi-component mixtures with a high CO_2 content and impurities, as shown on Table 2. The mixtures were supplied by BOC and certified based on gravimetric analysis in accordance with ISO 6142. The expanded uncertainties in the table were reported with 95% level of confidence by multiplying the standard uncertainties to the coverage factor of $k = 2$. In order to prevent condensation in the cylinders, they were kept in a laboratory environment with a temperature of ~293 K.

Various types of impurities with different concentrations were selected to represent the compositions of fluids expected in typical carbon capture, transport and storage schemes. The first multi component mixture, MIX 1, includes 94.9 mol% CO_2 with 5.1 mol% impurities (CH_4, N_2, H_2, O_2, CO and Ar). The second multi component mixture, MIX 2, contains 89.8 mol% CO_2 with 10.2 mol% of non-condensable gases N_2, O_2 and Ar as impurities. The third mixture, MIX 3, represents the composition of a high CO_2 content gas field in South East Asia with approximately 70 mol% CO_2, 20 mol% CH_4 and 10 mol% ethane, propane, i-butane and n-butane.

2.2. Equipment description

All viscosity measurements were conducted using an in-house designed and constructed set-up, a schematic view is shown in Figure 1 below. This setup was designed to have a maximum working pressure of 207 MPa and a maximum working temperature of 523.15 K. The set-up is located inside an oven, manufactured by BINDER GmbH, capable of being used at temperatures from 203.15 to 473.15 K.

The set-up is comprised of two small cylinders, with volumes of 25 cm^3, connected to each other through a capillary tube with a measured length of 14.78 m and a temperature-dependent calibrated internal diameter. An oscillating U tube densitometer Anton Paar DMA-HPM is connected to the set-up. Two three-way valves, one on top of one of the cylinders connected to capillary tube and one on top of the densitometer, are installed to inject the sample inside the cylinders, tube system and densitometer. The lower ends of the two cylinders are connected to opposite sides of a push-pull, motor driven mercury pump. This pump can move the sample fluid forwards and backwards between the two cylinders. There is

also a hand pump connected to the system to control the pressure of the entire fluid system by injection and withdrawal of mercury [30]. Two Quartzdyne pressure transducer (model: QS 30K-B) with a design pressure up to 207 MPa and accuracy of ±0.02 MPa [31] were connected to record the system pressure.

2.3. Measurement procedure

The capillary tube viscosity measurement method was employed to measure the viscosity of CO_2 systems with impurities. In each test, after applying vacuum to the entire system, the set-up was loaded with the sample mixtures through the injection point at the top of the densitometer. Then after disconnecting the sample cylinder from the system, the sample fluid was pushed through the capillary tube into the other cylinder using the push-pull mercury pump. The temperature of the system was set to the desired condition and the desired pressure was achieved using the hand pump. Once conditions had stabilized, and after isolating the densitometer by closing the related valve, the sample was pumped through the capillary tube at a number of flow rates. To ensure the consistency of the measurements, at each pressure, viscosities were determined at two or three different flow rates and at each flow rate three readings were logged, so the reported viscosity data in this study are an average of at least six or nine separate readings.

Pumping the sample fluid through the capillary tube by piston pump resulted in a dynamic differential pressure that was monitored and recorded until stable. Then the pump was stopped to record the static differential pressure. To ensure laminar flow conditions, Reynolds numbers were checked for the flow rates in which the measurements were performed. The modified Poiseuille equation [31], below, relates the pressure drop across the capillary tube to the viscosity, tube characteristics and also flow rate for compressible fluids through a tube:

$$q_1 = \frac{\pi D^4}{256 L \eta P_1}(P_1^2 - P_2^2) \qquad (01)$$

where, P_1 is the inlet pressure, P_2 is the outlet pressure, q_1 represents flow rate in the inlet pressure, L is length of the capillary tube (L=1477.8 cm), D refers to internal diameter of the capillary tube, η is viscosity of the flown fluid. The correction factors for the impact of the end-effect of the capillary tube and kinetic energy were negligible as the length of the capillary tube was long and the tests were performed as very low flow rates. At Dean Number, $De = 2Re\sqrt{r/R}$, [32] below 10.0 there are no significant effects (i.e., less than 0.2%) due to curved-pipe flow on the viscosity measurement [33][34][35]. At the maximum

Reynolds number of *Re* = 153.9 in this work, the Dean number of *De* = 9.7, shows that the effect of radial acceleration is less than 0.2%. The internal diameter of the tube was calibrated. The tube length changes with temperature but this had no noticeable influence on the measured viscosity. The maximum flow rate of 0.05 cm^3/s can be set using a push-pull pump with the accuracy of ±0.000005 cm^3/s. The very low flow rates of 0.0015, 0.0021 and 0.0030 cm^3/s were set in this work to ensure laminar flow in tube. The laminar flow conditions were checked by calculating the Reynolds number at each test. Typically, the Reynolds number was below 155. In addition, the ratio of the differential pressures to the set flow rates was calculated to ensure remains constant. At each set flow rate, a number of repetitions were performed until three consecutive reading gave less than 1% variation in the calculated viscosity.

2.4. Diameter Calibration procedure

The diameter of the capillary tube was calibrated using the viscosity data of pure CO_2 from REFPROP *v8.0* [36]. First, the pressure drop at desired pressures and temperatures were measured and the viscosity was calculated using assumed diameter and employing Hagen-Poiseuille equation. The assumed diameter, 0.029653 cm, was obtained from previous experiments for oil and gas fluids [37]. The new diameter for each isotherm was optimised by minimising the total deviations of experimental data from the viscosity data calculated by REFPROP *v8.0* [36]. Then, a correlation was found by fitting a linear trend line on the optimised diameters versus temperature. Figure 2 shows the trend line which fitted optimised diameter based on temperature. The calibrated diameter as a function of temperature can be found from Equation (02). The results from the diameter calibration can be found in Table 3.

$$D_{cal} = -0.000001107T + 0.0298 \quad (02)$$

where, D_{cal} is in cm and T is in K.

2.5. Viscosity validation

The viscosities of pure CO_2 were measured at two isotherms to validate the experimental procedure by comparing to experimental data obtained by Al-Siyabi et al. [38] and Pensado et al. [39]. They measured the viscosity of pure CO_2 at the desired temperatures at dense phase and at pressures up to 60 MPa. In this work, the viscosities of pure CO_2 were measured at two isotherms in gas, liquid and supercritical phases at pressures up to 150 MPa. The results are in good agreement with the literature. As can be seen in Table 4 and Figure 3, the

deviations of measurements for pure CO_2 from prediction values using CO_2-Pedersen method is within ±2% in gas, liquid and supercritical phases.

2.6. Viscosity measurement uncertainties

The type A and type B [40][41] uncertainty of each experimentally measured viscosity were calculated. The type A uncertainties of the viscosity measurements, $u_A(\eta)$, were determined from the standard deviations of up to 9 independent measurements. In general, the uncertainties of viscosity measurements in the gas phase and at low temperatures are higher than the dense phase CO_2 mixtures.

$$u_A(\eta) = \frac{s}{\sqrt{n}} \quad \text{and} \quad s = \sqrt{\frac{\sum_{i=1}^{n}(x_i - \bar{x})^2}{n-1}} \tag{03}$$

where,

s: Estimated standard deviation

$\bar{x}$: The mean of viscosity readings

u_A: Estimated standard uncertainty type A

n: number of measurements

The type B uncertainty of viscosity measurements were calculated according to the random error propagation theory [42].

$$u_c(\eta) = \pm\sqrt{\left[\left(\frac{\partial\eta}{\partial\Delta p}\right).d\Delta p\right]^2 + \left[\left(\frac{\partial\eta}{\partial q}\right).dq\right]^2 + \left[\left(\frac{\partial\eta}{\partial D}\right).dD\right]^2 + \left[\left(\frac{\partial\eta}{\partial L}\right).dL\right]^2} \tag{04}$$

In the above equation, the uncertainty of viscosity due to each variable, $\left(\frac{\partial\eta}{\partial M}\right)$, can be calculated from the following equation. The variable M could be pressure drop, Δp, flow rate, q, internal diameter, D, or tube length, L.

$$\left(\frac{\partial\eta}{\partial M}\right) = \frac{1}{2u(M)}\left(\eta_{M+u(M)} - \eta_{M-u(M)}\right) \tag{05}$$

The uncertainties of pressure drop, flow rate, diameter and tube length were estimated to be 0.00007 MPa, 0.000005 cm^3/s, 0.00005 cm and 5 cm, respectively. Standard uncertainties in temperature and pressure are $u(T)$ = 0.1 K [37] and $u(p)$ = 0.02 MPa [31][37].

3. Modelling

Numerous methods are available to predict the viscosities of mixtures including correlative model based on residual viscosity theory such as Lohrenz-Bray-Clark (LBC) [24], models based on the corresponding states theory such as Pedersen et al. [26], Aasberg-Petersen [28]

and SUPERTRAPP [27], a model based on the rigid-sphere theory, i.e., the Vesovic-Wakeham (VW) model [43][44][45][46], friction theory [47][48][49] and expanded fluid model [50][51].

This work was part of a joint industrial project (JIP). Therefore, mainly the existing models available in the engineering software packages which were the potential to modify them for the CO_2-rich systems were investigated. For instance, the Pedersen and LBC models are available in the PVTsim software package. In this work, four models were tested and developed to predict the viscosity of CO_2 dominated systems with impurities. Correlative model is based on the residual viscosity theory, i.e., Lohrenz-Bray-Clark (LBC) correlation [24]. This correlation is a fourth-degree polynomial equation in the reduced density which can be tuned to match experimental data. The predictive models are based on one-reference fluid corresponding states (CS) theory, i.e., Pedersen [26], two-reference fluid corresponding states (CS2) theory, i.e., Aasberg-Petersen [28], based on extended corresponding states (ECS) theory, i.e., SUPERTRAPP [27].

4.1 Residual viscosity theory

Due to the simplicity, flexibility and consistency, the most common empirical viscosity calculation method for both gases and liquids in petroleum industry which widely in use in compositional simulators, based on the residual viscosity concept, is a correlation derived by Jossi et al. [52] for pure fluids. The concept of residual viscosity is based on the experimental observation that the viscosity differences between the dense phase and dilute gas at a specific temperature is a function of its density [52]. This correlation is mostly referred as Lohrenz-Bray-Clark (LBC) correlation in the oil and gas industry. Lohrenz et al. [24] extended the JST method [52] for calculating the viscosity of mixtures of naturally occurring hydrocarbons. The LBC correlation is a fourth-degree polynomial equation in the reduced density, $\rho_r = {\rho}/{\rho_c}$:

$$[(\eta - \eta^*)\xi + 10^{-4}]^{\frac{1}{4}} = a_1 + a_2\rho_r + a_3\rho_r^2 + a_4\rho_r^3 + a_5\rho_r^4 \quad (06)$$

In this equation, the viscosity of dilute gas, η^*, were obtained from a mixing rule proposed by Herning et al. [53]. The mixing rule is based on the dilute component viscosity for each component, η_i^*, as a function of reduced temperature, T_{ri}, which proposed by Stiel and Thodos [54]. A mixing rule also were applied by Lohrenz et al. [24] for ξ, the viscosity reducing parameter. The constants a_1 to a_5, available from Table 5, were adjusted by Jossi et al. [52] using 11 pure compounds for reduced densities of 0.02 to 3.0. The compounds were:

carbon dioxide, sulphur dioxide, non-condensable gases (oxygen, argon, nitrogen) and hydrocarbons (methane, ethane, propane, i-butane, n-butane, and n-pentane).

It should be mentioned that the model predicts the natural gas and light hydrocarbons mixtures viscosity with a reasonable accuracy. This could be due to the fact that the parameters of the model were adjusted using light hydrocarbons. Dandekar et al. [55] showed that the model predicts the viscosity of hydrocarbon systems with a reasonable range of accuracy when the reduced densities are less than 2.5. The model under-predicts the fluid viscosity significantly for systems with reduced densities above 2.5. They also have modified the model for heavier hydrocarbon systems by introducing reduced temperature and molecular weight [55]. Furthermore, the residual viscosity in the main equation is supposed to be a function of reduced temperature. But, as demonstrated by Vogel et al. [56] for propane, a temperature dependency can be observed for reduced densities above 3. A similar behaviour can be expected for other systems at higher reduced densities.

In this work, the parameters a_1 to a_5 were tuned to match to the experimental viscosity data of CO_2 systems with impurities. The density of the mixture can be calculated by any equation of state (EoS), for instance, Peng-Robinson (PR EoS) [57]. However, as the original model developed based on the experimental density, the accuracy of the model significantly depends on the input density. In this work, an in-house thermodynamic properties prediction package, HWPVT [58][59][60], was used to calculate the mixture density using the PR [57] with the CO_2 volume correction [23][29][60] (PR-CO_2 EoS) for CO_2-rich systems.

4.2 Corresponding states theory with one reference fluid

One of the well-known semi-theoretical approaches to predict the transport properties of fluids is corresponding states (CS) theory. The principle of corresponding states arises from the fact that properties of many fluids are similar as a function of critical temperature and critical density [21]. The Pedersen equation [26] for prediction of the viscosities of hydrocarbon fluids can be obtained from the following equation:

$$\eta_{mix}(P,T) = \frac{\left(\frac{P_{c,mix}}{P_{c,0}}\right)^{\frac{2}{3}}\left(\frac{M_{mix}}{M_0}\right)^{\frac{1}{2}}\left(\frac{\alpha_{mix}}{\alpha_0}\right)}{\left(\frac{T_{c,mix}}{T_{c,0}}\right)^{\frac{1}{6}}}\eta_0(P_0,T_0) \qquad (07)$$

In the modified model, CO_2-Pedersen, the reference fluid was modified by changing from methane to carbon dioxide [25] for the high CO_2 content systems. The model was well described in the previous work [29].

4.3 Corresponding states theory with two reference fluids

A viscosity model based on corresponding states theory with two reference fluids was proposed by Aasberg-Petersen et al. [28] to predict the viscosity of both gases and liquid systems for hydrocarbons. They have selected methane [61] and n-decane add reference here as the reference fluids. The mixture viscosity in this model can be obtained from the following equation:

$$\eta_{mix} = \eta_{C,mix} \frac{\eta_1(T_1, P_1)}{\eta_{C,1}} \left[\frac{\eta_2(T_2, P_2).\eta_{C,1}}{\eta_1(T_1, P_1).\eta_{C,2}} \right]^{K_{CS}} \quad (08)$$

where K_{CS} is an interpolation parameter function of molecular weights of the mixture and reference fluids. Et-Tahir et al. [62] investigated the effect of interpolation parameter, K_{CS}, by introducing other parameters, i.e., acentric factor, critical pressure and temperature, as shown on the equation below.

$$K_{CS} = \frac{1}{4}\left(\frac{M_{w,mix} - M_{w,1}}{M_{w,2} - M_{w,1}} + \frac{\omega_{mix} - \omega_1}{\omega_2 - \omega_1} + \frac{P_{C,mix} - P_{C,1}}{P_{C,2} - P_{C,1}} + \frac{T_{C,mix} - T_{C,1}}{T_{C,2} - T_{C,1}} \right) \quad (9)$$

In this work, the K_{CS} proposed by Et-Tahir et al. [62] were employed. Additionally, the reference fluids, were changed from methane and n-decane to methane [61] and carbon dioxide [25].

4.4 Extended corresponding states (ECS) theory

The method was proposed by Hanley [63] and also by Mo & Gubbins [64][65]. It led to a computer programme known as TRAPP (TRAnsport Properties Prediction) [66]. The method is also the basis for NIST Standard Reference Database 4 (SUPERTRAPP, [27]). The method can predict viscosity and thermal conductivity of pure fluids and their mixtures over the entire phase range from gas to dense liquid.

The original version of the TRAPP method [66] was used to estimate the viscosity and thermal conductivity of fluids and their mixtures and employed methane as a reference fluid. In the most recent version, propane is the reference fluid. Other reference fluids can be chosen. For example, Huber and Ely [67] use R134a as the reference fluid to predict transport properties of refrigerants. In this method, the residual viscosity of the mixture, which is related to the residual viscosity of the reference fluid, is given by [66]:

$$\eta_m - \eta_m^0 = F_{\eta m}[\eta^R - \eta^{R0}] + \Delta\eta^{ENSKOG} \quad (10)$$

The term $\eta^R - \eta^{R0}$ is for the residual viscosity of the reference fluid which should be evaluated at the corresponding state point of T_0 and ρ_0 (not at T and ρ). The term $\Delta\eta^{ENSKOG}$ accounts for size differences based on a hard sphere assumption by Ely et al. [66].

$$T_0 = \frac{T}{f_m} \quad \text{and} \quad \rho_0 = \rho h_m \tag{11}$$

The residual viscosity of the reference fluid, propane, can be determined from a method given by Younglove and Ely [68]. In this work, Carbon Dioxide with the viscosity data published by Fenghour et al. [25] was used as the reference fluid. Similar to the LBC and CO_2-LBC models, the densities of the mixtures were predicted using the PR-CO_2 EoS.

4. Results and discussions

4.1. *Experimental and modelling results*

Most of the available viscosity data are in the gas phase and atmospheric pressure as discussed in the literature review. There are large gaps between the available experimental data and the requirements for the viscosity of CO_2-rich systems in carbon capture, transport and storage. As the operationally and economically preferred scenarios to transport captured carbon dioxide in CCS is by pipeline in the dense liquid / supercritical phase, availability of robust viscosity data at higher pressure and in the dense phase is of crucial importance.

The viscosities of pure CO_2 for calibration purposes, multi-component mixtures of MIX 1 (with 5% impurity), MIX 2 (with 10% impurity) and MIX 3 (with 30% impurity) were measured using the capillary tube technique. For calibration purposes, viscosities of pure CO_2 were measured over a wide range of pressure, temperature and fluid conditions. A total of 62 points for pure CO_2 and 153 viscosity data points for MIX 1, MIX 2 and MIX 3 were measured, of which 37 points were in the gas phase, 61 points were in the liquid phase and 55 points were in the supercritical phase. Average and maximum of the type A and type B of estimated standard uncertainties of viscosity for each material was reported in Table 9. As can be seen, the average type A and B of uncertainties are 0.4% and 0.8%, respectively.

The experimental data were then employed to tune the correlative LBC and CO_2-LBC models and to evaluate the predictive models. The predictive models in this work are based on the corresponding states (CS) theory models. One reference fluid models are Pedersen and CO_2-Pedersen; two reference fluid models are Aasberg-Petersen (CS2) and CO_2-CS2 models and two models base on extended corresponding states (ECS) theory, SUPERTRAPP and CO_2-SUPERTRAPP models. The experimental results at corresponding pressure and temperature with the estimated uncertainties are shown in Tables 6 to 8 and Figures 4 to 6. The summary

of the Absolute Average Deviations (AADs) for each mixture in gas, liquid and supercritical phases are presented in Table 10 and Table 11 for both correlative and predictive models, respectively.

4.2. Discussions on the correlative models

The LBC correlation based on the residual viscosity theory due to the simplicity is one of the most common correlations in the oil and gas industry to calculate viscosity of fluids. CO_2-LBC model is the LBC correlation with new tuned parameters using the experimental viscosity data of CO_2-rich systems generated in this work. The LBC and CO_2-LBC parameters are available in Table 5. As can be seen, the new tuned parameters for the CO_2-LBC model are 0.10799, 0.035452, 0.021269, -0.013284 and 0.0034455 for a_1 to a_5, respectively.

The viscosity predicted by the LBC models is a strong function of the density of the mixture. Therefore, the effect of density correction on the viscosity predicted by the LBC models were investigated. As can be seen in Table 10, by comparing columns 7 and 8, the AAD for the LBC correlation using PR EoS [57] without CO_2 density correction is 21.2% while after tuning and applying the predicted mixture density using the same equation of state with CO_2 volume correction (CO_2-LBC) is 9.2%. The application of CO_2 volume correction was discussed in previous work [29]. The minimum and maximum AADs for the original LBC correlation with density correction are 7.3% and 13.6% for MIX 1 and MIX 3, respectively while those are 6.7% and 16.2% for MIX 1 and MIX 3, respectively, using the CO_2-LBC with density correction.

4.2.1. Effect of tuning parameters and mixture density correction

In the modelling part, Equation (06) is the main equation for the LBC correlation which is function of the mixture density and five constant parameters. The parameters for the LBC correlation are presented in Table 5. There are two methods to improve the prediction of the LBC correlation. One of the most common methods for this purpose is to tune the parameters to match to experimental data. Improving the mixture density prediction can be another method [23][69]. The effect of tuning can be analysed from Table 10. As can be seen, the AAD was reduced from 9.9% to 9.2% when the density correction is considered (comparing columns 5 and 6), while it was reduced from 21.2% to 20.1% without applying density correction term (comparing columns 7 and 8). The effect of mixture density on viscosity prediction can be realised by comparing columns 5 and 7 for original LBC and 6 and 8 for

CO_2-LBC models. The table shows that applying density correction term in the original LBC model can reduce the AAD from 21.2% to 9.9% while those are reducing from 20.1% to 9.2% for the CO_2-LBC model. By comparing these two improving methods, it can be observed that applying mixture density correction term would reduce the AAD significantly compared to adjusting the tuning parameters a_1-a_5. Figure 7 graphically show the effects of tuning parameters and density correction in LBC and CO_2-LBC models.

4.2.2. Predictions of the models in different phases

Table 10 also can be used to compare the accuracy of the models prediction in different fluid phases. In the gas phase, the AADs are high for both original LBC and modified CO_2-LBC, i.e., 12.8% and 12.9%, respectively. As can be seen, the accuracy of models were not increased neither using tuned parameters nor applying the density correction term in the gas phase. It seems reasonable as volume correction term has mostly an effect on the density in the dense phase, i.e., liquid or supercritical phase. In the liquid or supercritical phases, the AAD reduces significantly from 30.7% to 8.4% for the LBC model and from 25.5% to 7.1% for the CO_2-LBC model by applying CO_2 volume correction term in liquid phase. Those are reducing from 16.4% to 9.6% and from 18.8% to 9.1% for LBC and CO_2-LBC models in the supercritical phase, respectively. The effect of tuning parameters in the liquid phase can be observed by comparing columns 5 and 6 or columns 7 and 8 with and without considering density correction. The AAD reduces from 8.4% to 7.1% when the density correction term is applied while it reduces from 30.7% to 25.5% without density correction. Tuning parameters also can reduce the AAD from 9.6% to 9.1% with applying density correction term in the supercritical phase, while it increases the AAD from 16.4% to 18.8% without density correction.

4.3. Discussions on the predictive models

Predictive models in this work are based on corresponding states (CS) theory with one reference fluid, Pedersen and CO_2-Pedersen models, with two reference fluids, Aasberg-Petersen (CS2) and CO_2-CS2 models, and extended corresponding states (ECS) theory, SUPERTRAPP and CO_2-SUPERTRAPP models. The models were described in the modelling part. The AAD for each model were summarised in Table 11. As can be seen, the CO_2-Pedersen model has the lowest AAD of 3.8% while it is 9.4% for the original Pedersen model. The significant reduction in the AAD can show the effect of reference fluid selection on the viscosity prediction accuracy by corresponding states theory models for different

systems. In this work, instead of methane in the original Pedersen model, the CO_2 was selected as the reference fluid in the CO_2-Pedersen model. The original Aasberg-Petersen model with two reference fluids (methane and n-decane) has the AAD of 14.4% which is relatively high for CO_2-rich systems. However, changing the n-decane to carbon dioxide could reduce the AAD to 5.3%. The CO_2-SUPERTRAPP model also has the AAD of 4.6% which is the best models after CO_2-Pedersen model. Figure 8 compares the deviations of models based on the corresponding states theory, i.e., Pedersen, CO_2-Pedersen, Aasberg-Petersen (CS2) and CO_2-CS2.

4.3.1. The effect of mixture density on the viscosity modelling by CO2-SUPERTRAPP

Unlike CO_2-Pedersen model which only requires the density of reference fluid to predict the mixture viscosity, viscosity prediction of SUPERTRAPP models are a function of mixture density. In modelling the viscosity using SUPERTRAPP models, the residual viscosity of any mixture is related to residual viscosity of the reference fluid at a corresponding state point of (ρ_0, T_0). According to description of the model, also can be seen on the Equation (10), the viscosity of reference fluid should be evaluated at temperature T_0 and density ρ_0, which density ρ_0 is a function of the mixture density. However, the mixture density has a significant effect on the mixture viscosity in SUPERTRAPP models. Table 11 and Figure 9 show this effect for all conducted tests.

As can be seen, using the modified density for the CO_2-rich systems reduces the overall absolute average deviation from 16.3% to 7.4% using the original SUPERTRAPP model. This amount reduces from 9.4% to 4.6% using the CO_2-SUPERTRAPP model. As applying the density correction term, mostly increases the accuracy of densities in the dense liquid / supercritical phases, this effect can be seen on the viscosity prediction accuracy in these phases. For instance, applying the density correction term in the original SUPERTRAPP model reduces the AAD from 22.8% to 6.8% and from 15.9% to 8.8% in the liquid and supercritical phases, respectively. These quantities in the CO_2-SUPERTRAPP model reduce from 13.6% to 5.2% and from 6.8% to 2.9% in the liquid and supercritical phases, respectively.

4.3.2. Prediction of the models in different phases

As can be seen from Table 11, in gas phase, most of the models, except Aasberg-Petersen, have acceptable viscosity prediction for CO_2 fluids containing impurities. The lowest AAD of 2.1% in gas phase is for the CO_2-CS2 model. In the liquid phase, CO_2-Pedersen has the

lowest AAD of 4.5% while CO_2-SUPERTRAPP has the lowest AAD of 2.9% in the supercritical phase. These models are the most accurate viscosity prediction models in the gas or dense phases for CO_2 systems with impurities.

4.4. The effect of different impurities on viscosity of pure CO_2

The presence of impurities can affect the viscosity of pure CO_2. Table 12 shows the viscosity reduction in the dense phase and viscosity increase in the gas phase for each tested mixtures at different temperatures. The effect of impurities on the viscosity of pure CO_2 also can be observed in Figure 10 for all tested pressure ranges at constant temperature of 323.15 K (50 °C). In this figure, the experimental viscosity data and modelling predictions using CO_2-Pedersen model for each system are reported at 323.15 K (50 °C). As expected, the presence of the tested systems with impurities caused a decrease in the viscosity at higher pressure ranges, i.e., in liquid and supercritical phases. This reduction can be explained by a reduction in density and molecular weight of the tested mixtures. The reduction in viscosity of pure CO_2 in the presence of impurities for each system can be seen in Figure 10. The lowest viscosity reduction of 9.6% is for MIX 1 with 4.4% impurities, while the highest reduction of 30.9% is for those of MIX 3 with almost 30.01% impurities.

In gas phase, the presence of impurities increased viscosity (which was expected). The increase in viscosity is due to the increase in kinetic energy of the system. The lowest viscosity increase of 0.9% is for MIX 1, while that is 8.9% for MIX 3 which has the highest viscosity increase due to the presence of impurities.

The viscosity changes from pure CO_2 for MIX 1 at different temperatures were shown in Figure 11. The highest reduction in the viscosity of MIX 1 is happening nearby critical point, at 298.15 K (25 °C) and at pressures around 8 MPa. At high temperatures in supercritical phase, viscosity reduction from pure CO_2 would be smooth. As could be seen in Figure 11, the high reduction of 25% in viscosity of pure CO_2 due to the presence of MIX 1 impurities were measured at 323.15 K (50 °C) at pressures around 9 MPa.

5. Conclusions

Estimation of transport properties is imperative to analyse fluid flow behaviour and heat transfer from fluids to the environment. Viscosity is a key transport property for pipeline systems as well as sub-surface and process systems. This work has focussed on the viscosity of CO_2-rich mixtures. Both experimental measurements and modelling practices are covered. The viscosities of proposed mixtures were measured in the gas, liquid and supercritical phases. It was concluded that, as expected, the uncertainty of measurements in the gas phase is higher than dense liquid / supercritical phases. Results from the measured viscosity data showed that the presence of the impurities reduces the viscosity of the mixture compared to pure carbon dioxide in the dense liquid / supercritical phases. Conversely, the viscosity increases in the gas phase due to the presence of impurities. The extent of the reduction / increase depends on the type and concentration of the impurity. Generally, it can be concluded that the lighter the molecule, the higher the reduction in the viscosity of pure CO_2.

Extensive tuning and modifications were also performed on the existing viscosity models available in the literature as well as in the oil and gas industry and commercial packages. The obtained viscosity data were employed to tune the Lohrenz-Bray-Clarck, (LBC) model, to match the experimental data. New parameters were calculated by optimising the parameters and the model with the specific set of parameters for CO_2 fluids was renamed CO_2-LBC. The absolute average deviations (AAD) were calculated for both models and it was concluded that the CO_2-LBC model has a lower AAD than original LBC as expected. The prediction improvement could be seen on the gas phase as well as in the dense liquid / supercritical phases. Moreover, the effect of density correction on the viscosity prediction using LBC and CO_2-LBC was investigated. The conclusion comes from comparing the AAD of the models from experimental data. By applying the CO_2 volume correction to the PR EoS, the AAD for the CO_2-LBC model were reduced from 20.1% to 9.2% while that of original LBC reduced from 21.2% to 9.9%.The conclusions drawn during the course of this study show that as the correlative LBC models are strong function of the mixture density, improving the density prediction using the CO_2 volume correction can improve the viscosity predictions significantly. This improvement is more evident in the dense liquid / supercritical phases as the CO_2 volume correction is suitable to improve the density prediction in the dense phase. In the gas phase, as mentioned above, density predictions was not effected by applying the CO_2 volume correction.

The predictive models investigated in this work were based on the corresponding states theory. The one reference fluid corresponding state model, Pedersen, was modified by selecting pure CO_2 as a reference fluid for CO_2-rich systems. It is concluded that the modified model, CO_2-Pedersen, improved the viscosity predictions significantly. The absolute average deviation was reduced from 9.4% to 3.8%. The improvements in the viscosity predictions were in all phases. The two reference fluid corresponding state model, Aasberg-Petersen, was also modified for CO_2-rich systems by changing the reference fluid from n-decane to carbon dioxide. The results show that the new model after modification, CO_2-CS2, predicts with greater accuracy particularly for hydrocarbon – carbon dioxide systems in the gas phase. The SUPERTRAPP model, based on extended corresponding states (ECS) theory, was also modified by changing the reference fluid from propane to carbon dioxide. It was concluded that the new model, CO_2-SUPERTRAPP, accurately predicts the viscosity of CO_2 systems in the supercritical phase. The AAD of this model in the supercritical phase for the investigated mixtures is 2.9%. Overall, the original SUPERTRAPP model over-predicts the viscosity while CO_2-SUPERTRAPP model under-predicts the viscosity. In addition, the effect of density correction on viscosity prediction using this model was also investigated. The SUPERTRAPP model, similar to LBC, is a strong function of mixture density. The conclusion from the results is that applying the CO_2 volume correction can improve the viscosity prediction in the dense liquid / supercritical phase significantly. As a result, CO_2-Pedersen is recommended to predict the viscosity of CO_2-rich systems.

6. Acknowledgements

This work is part of the first phase of the JIP project" Impact of Common Impurities on Carbon Dioxide Capture, Transport and Storage" [29] was conducted jointly at the institute of petroleum engineering at Heriot-Watt University in UK and centre for thermodynamic process at MINES ParisTech in France from 2011 - 2014. The objective of the project was measuring thermophysical properties i.e., phase equilibira, hydrates [70], frost point measurement, density [23][60][71], viscosity, interfacial tension [72], solubility [73][74][75] and pH. The authors would like to gratefully acknowledge the sponsors for their support: Chevron, GALP Energia, Linde AG Engineering Division, OMV, Petroleum Expert, Statoil, TOTAL and National Grid Carbon Ltd.

REFERENCES

[1] W. Jung and J.-P. Nicot, "Impurities in CO2 - Rich Mixtures Impact CO2 Pipeline Design: Implications for Calculating CO2 Transport Capacity," in *Proceedings of SPE International Conference on CO2 Capture, Storage, and Utilization*, 2010.

[2] J.-Y. Lee, T. C. Keener, and Y. J. Yang, "Potential Flue Gas Impurities in Carbon Dioxide Streams Separated from Coal-Fired Power Plants," *J. Air Waste Manage. Assoc.*, vol. 59, no. 6, pp. 725–732, Feb. 2012.

[3] R. T. J. Porter, M. Fairweather, M. Pourkashanian, and R. M. Woolley, "The range and level of impurities in CO2 streams from different carbon capture sources," *Int. J. Greenh. Gas Control*, vol. 36, pp. 161–174, May 2015.

[4] S.-S. Fan, G.-J. Chen, Q.-L. Ma, and T.-M. Guo, "Experimental and modeling studies on the hydrate formation of CO2 and CO2-rich gas mixtures," *Chem. Eng. J.*, vol. 78, no. 2, pp. 173–178, 2000.

[5] L. Zhang, L. Yang, J. Wang, J. Zhao, H. Dong, M. Yang, Y. Liu, and Y. Song, "Enhanced CH4 recovery and CO2 storage via thermal stimulation in the CH4/CO2 replacement of methane hydrate," *Chem. Eng. J.*, vol. 308, pp. 40–49, 2017.

[6] J. Gale, C. Hendriks, W. Turkenberg, J. Wang, D. Ryan, E. J. Anthony, N. Wildgust, and T. Aiken, "Effects of impurities on CO2 transport, injection and storage," *Energy Procedia*, vol. 4, pp. 3071–3078, 2011.

[7] H. Li, J. P. Jakobsen, Ø. Wilhelmsen, and J. Yan, "PVTxy properties of CO2 mixtures relevant for CO2 capture, transport and storage: Review of available experimental data and theoretical models," *Appl. Energy*, vol. 88, no. 11, pp. 3567–3579, Nov. 2011.

[8] M. M. J. Knoope, A. Ramírez, and A. P. C. Faaij, "A state-of-the-art review of techno-economic models predicting the costs of CO2 pipeline transport," *Int. J. Greenh. Gas Control*, vol. 16, pp. 241–270, Aug. 2013.

[9] H. Li, Ø. Wilhelmsen, Y. Lv, W. Wang, and J. Yan, "Viscosities, thermal conductivities and diffusion coefficients of CO2 mixtures: Review of experimental data and theoretical models," *Int. J. Greenh. Gas Control*, vol. 5, no. 5, pp. 1119–1139, Sep. 2011.

[10] M. Nazeri, M. M. Maroto-Valer, and E. Jukes, "Performance of Coriolis flowmeters in CO2 pipelines with pre-combustion, post-combustion and oxyfuel gas mixtures in carbon capture and storage," *Int. J. Greenh. Gas Control*, vol. 54, pp. 297–308, 2016.

[11] "European CCS Directive – Directive of the European Parliament and of the council

on the geological Storage of Carbon Dioxide Amending Council Directives 85/337/EEC, 96/61/EC, Directives 2000/60/EC, 2001/80/EC, 2004/35/EC, 2006/12/EC."

[12] DNV-RP-J202, "Design and operation of CO2 pipelines," 2010.

[13] C.-W. Lin, M. Nazeri, A. Bhattacharji, G. Spicer, and M. M. Maroto-Valer, "Apparatus and method for calibrating a Coriolis mass flow meter for carbon dioxide at pressure and temperature conditions represented to CCS pipeline operations," *Appl. Energy*, vol. 165, pp. 759–764, Mar. 2016.

[14] L. Hunter and G. Leslie, "A Study of Measurement Issues for Carbon Capture and Storage (CCS)," *TUV NEL Rep. 2009/54, NEL, East Kilbride*, 2009.

[15] G. J. Collie, M. Nazeri, A. Jahanbakhsh, C.-W. Lin, and M. M. Maroto-Valer, "Review of flowmeters for carbon dioxide transport in CCS applications," *Greenh. Gases Sci. Technol.*, pp. 1–19, Dec. 2016.

[16] C. Hardie, "Developing Measurement Facilities for Carbon Capture and Storage," *Meas. Control*, vol. 46, no. 2, pp. 44–49, Mar. 2013.

[17] A. Chapoy, R. Burgass, B. Tohidi, J. M. Austell, and C. Eickhoff, "Effect of Common Impurities on the Phase Behavior of Carbon-Dioxide-Rich Systems: Minimizing the Risk of Hydrate Formation and Two-Phase Flow," *SPE J.*, vol. 16, no. 4, pp. 921–930, Dec. 2011.

[18] TUVNEL, "Measurement of CO2 throughout the carbon capture and storage (CCS) chain," 2009.

[19] S. T. McCoy and E. S. Rubin, "An engineering-economic model of pipeline transport of CO2 with application to carbon capture and storage," *Int. J. Greenh. Gas Control*, vol. 2, no. 2, pp. 219–229, Apr. 2008.

[20] E. Hendriks, G. M. Kontogeorgis, R. Dohrn, J.-C. de Hemptinne, I. G. Economou, L. F. Žilnik, and V. Vesovic, "Industrial Requirements for Thermodynamics and Transport Properties," *Ind. Eng. Chem. Res.*, vol. 49, no. 22, pp. 11131–11141, Nov. 2010.

[21] C. A. Millat, J., Dymond, J.H., Nieto de Castro, *Transport Properties of Fluids, Their Correlation, Prediction and Estimation*. Cambridge University Press, IUPAC, 2005.

[22] Z. K. S. Al-Siyabi, "The contact angle, interfacial tension and viscosity of reservoir fluids : experimental data and modelling." Petroleum Engineering, 2000.

[23] M. Nazeri, A. Chapoy, R. Burgass, and B. Tohidi, "Measured densities and derived thermodynamic properties of CO2-rich mixtures in gas, liquid and supercritical phases

from 273K to 423K and pressures up to 126MPa," *J. Chem. Thermodyn.*, vol. 111, pp. 157–172, 2017.

[24] J. Lohrenz, B. G. Bray, and C. R. Clark, "Calculating Viscosities of Reservoir Fluids From Their Compositions," *J. Pet. Technol.*, vol. 16, no. 10, pp. 1171–1176, Apr. 1964.

[25] Fenghour; A.; Wakeham; W.A.; Vesovic;, "The Viscosity of Carbon Dioxide," *J. Phys. Chem. Ref. Data, Vol. 27, No. 1,* 1998. .

[26] K. S. Pedersen and A. Fredenslund, "An improved corresponding states model for the prediction of oil and gas viscosities and thermal conductivities," *Chem. Eng. Sci.*, vol. 42, no. 1, pp. 182–186, Jan. 1987.

[27] J. F. Huber, M. L. and Ely, "NIST Standard Rejerence Database 4: NIST Thermophysical Properties of Hydrocarbon Mixtures," *U.S. Department of Commerce, Washington, DC*, 1990. .

[28] K. Aasberg-Petersen, K. Knudsen, and A. Fredenslund, "Prediction of viscosities of hydrocarbon mixtures," *Fluid Phase Equilibria*, vol. 70. pp. 293–308, 1991.

[29] A. Chapoy, M. Nazeri, M. Kapateh, R. Burgass, C. Coquelet, and B. Tohidi, "Effect of impurities on thermophysical properties and phase behaviour of a CO2-rich system in CCS," *Int. J. Greenh. Gas Control*, vol. 19, pp. 92–100, Nov. 2013.

[30] K. Kashefi, A. Chapoy, K. Bell, and B. Tohidi, "Experimental Study: The Impact of Dissolved Water on the Viscosity of Reservoir Fluids at HPHT Conditions," *J. Chem. Eng. Data*, vol. 60, no. 3, pp. 674–682, Mar. 2015.

[31] B. Tohidi, R. W. Burgass, A. Danesh, and A. C. Todd, "Viscosity and Density of Methane + Methylcyclohexane from (323 to 423) K and Pressures to 140 MPa," *J. Chem. Eng. Data*, vol. 46, no. 2, pp. 385–390, Mar. 2001.

[32] W. R. Dean, "XVI. *Note on the motion of fluid in a curved pipe*," *London, Edinburgh, Dublin Philos. Mag. J. Sci.*, vol. 4, no. 20, pp. 208–223, Jul. 1927.

[33] W. A. Wakeham, A. (Akira) Nagashima, J. V. Sengers, and International Union of Pure and Applied Chemistry. Commission on Thermodynamics., *Measurement of the transport properties of fluids, Experimental Thermodynamics, Volume III*. Blackwell Scientific Publications, 1991.

[34] A. G. Clarke and E. B. Smith, "Low-Temperature Viscosities of Argon, Krypton, and Xenon," *J. Chem. Phys.*, vol. 48, no. 9, pp. 3988–3991, May 1968.

[35] R. A. Dawe, "A Method for Correcting Curved-Pipe Flow Effects Occurring in Coiled Capillary Viscometers," *Rev. Sci. Instrum.*, vol. 44, no. 9, pp. 1231–1233, Sep. 1973.

[36] E. W. Lemmon, M. L. Huber, and M. O. McLinden, "NIST standard reference database 23: reference fluid thermodynamic and transport properties – REFPROP version 8.0. Gaithersburg: National Institute of Standards and Technology, Standard Reference Data Program." 2007.

[37] K. Kashefi, A. Chapoy, K. Bell, and B. Tohidi, "Viscosity of binary and multicomponent hydrocarbon fluids at high pressure and high temperature conditions: Measurements and predictions," *J. Pet. Sci. Eng.*, vol. 112, pp. 153–160, Dec. 2013.

[38] I. Al-Siyabi, "Effect of Impurities on CO2 Stream Properties, PhD Thesis," Institute of Petroleum Engineering, Heriot-Watt University, Edinburgh, 2013.

[39] A. S. Pensado, A. A. H. Pádua, M. J. P. Comuñas, and J. Fernández, "Viscosity and density measurements for carbon dioxide+pentaerythritol ester lubricant mixtures at low lubricant concentration," *J. Supercrit. Fluids*, vol. 44, no. 2, pp. 172–185, Mar. 2008.

[40] B. N. Taylor and C. E. Kuyatt, *Guidelines for Evaluating and Expressing the Uncertainty of NIST Measurement Results*. NIST, 1994.

[41] S. Bell, *Measurement Good Practice Guide No. 11 (Issue 2), A Beginner's Guide to Uncertainty of Measurement*. National Physical Laboratory, 2001.

[42] "JCGM 100:2008, GUM 1995 with minor corrections, Evaluation of measurement data — Guide to the expression of uncertainty in measurement, First edition September 2008."

[43] V. Vesovic and W. A. Wakeham, "Prediction of the viscosity of fluid mixtures over wide ranges of temperature and pressure," *Chem. Eng. Sci.*, vol. 44, no. 10, pp. 2181–2189, 1989.

[44] V. Vesovic and W. A. Wakeham, "The prediction of the viscosity of dense gas mixtures," *Int. J. Thermophys.*, vol. 10, no. 1, pp. 125–132, Jan. 1989.

[45] M. J. Assael, N. K. Dalaouti, and V. Vesovic, "Viscosity of Natural-Gas Mixtures: Measurements and Prediction," *Int. J. Thermophys.*, vol. 22, no. 1, pp. 61–71, 2001.

[46] V. Vesovic, "Predicting the Viscosity of Natural Gas," *Int. J. Thermophys.*, vol. 22, no. 2, pp. 415–426, 2001.

[47] S. E. Quiñones-Cisneros, C. K. Zéberg-Mikkelsen, and E. H. Stenby, "The friction theory (f-theory) for viscosity modeling," *Fluid Phase Equilib.*, vol. 169, no. 2, pp. 249–276, Mar. 2000.

[48] S. P. Tan, H. Adidharma, B. F. Towler, and M. Radosz, "Friction Theory and Free-Volume Theory Coupled with Statistical Associating Fluid Theory for Estimating the

Viscosity of Pure n -Alkanes," *Ind. Eng. Chem. Res.*, vol. 44, no. 22, pp. 8409–8418, Oct. 2005.

[49] C. K. Zéberg-Mikkelsen, S. E. Quiñones-Cisneros, and E. H. Stenby, "VISCOSITY PREDICTION OF CARBON DIOXIDE + HYDROCARBON MIXTURES USING THE FRICTION THEORY," *Pet. Sci. Technol.*, Feb. 2007.

[50] M. A. Satyro and H. W. Yarranton, "Expanded fluid-based viscosity correlation for hydrocarbons using an equation of state," *Fluid Phase Equilib.*, vol. 298, no. 1, pp. 1–11, 2010.

[51] H. Motahhari, M. A. Satyro, S. D. Taylor, and H. W. Yarranton, "Extension of the Expanded Fluid Viscosity Model to Characterized Oils," *Energy & Fuels*, vol. 27, no. 4, pp. 1881–1898, Apr. 2013.

[52] J. A. Jossi, L. I. Stiel, and G. Thodos, "The viscosity of pure substances in the dense gaseous and liquid phases," *AIChE J.*, vol. 8, no. 1, pp. 59–63, Mar. 1962.

[53] L. Herning, F., Zipperer, "Calculation of the viscosity of technical gas mixtures from the viscosity of the individual gases," *das Gas- und Wasserfach*, vol. 79, pp. 49–54, 69–73, 1936.

[54] L. I. Stiel and G. Thodos, "The viscosity of nonpolar gases at normal pressures," *AIChE J.*, vol. 7, no. 4, pp. 611–615, Dec. 1961.

[55] A. Y. Dandekar, "Interfacial Tension and Viscosity of Reservoir Fluids, PhD thesis," Heriot-Watt University, 1994.

[56] E. Vogel, C. Küchenmeister, E. Bich, and A. Laesecke, "Reference Correlation of the Viscosity of Propane," *J. Phys. Chem. Ref. Data*, vol. 27, no. 5, p. 947, Sep. 1998.

[57] D.-Y. Peng and D. B. Robinson, "A New Two-Constant Equation of State," *Ind. Eng. Chem. Fundam.*, vol. 15, no. 1, pp. 59–64, Feb. 1976.

[58] A. Chapoy, H. Haghighi, R. Burgass, and B. Tohidi, "On the phase behaviour of the (carbon dioxide+water) systems at low temperatures: Experimental and modelling," *J. Chem. Thermodyn.*, vol. 47, pp. 6–12, Apr. 2012.

[59] H. Haghighi, A. Chapoy, R. Burgess, and B. Tohidi, "Experimental and thermodynamic modelling of systems containing water and ethylene glycol: Application to flow assurance and gas processing," *Fluid Phase Equilib.*, vol. 276, no. 1, pp. 24–30, Feb. 2009.

[60] M. Nazeri, A. Chapoy, A. Valtz, C. Coquelet, and B. Tohidi, "Densities and derived thermophysical properties of the 0.9505 CO2+0.0495 H2S mixture from 273 K to 353 K and pressures up to 41 MPa," *Fluid Phase Equilib.*, vol. 423, pp. 156–171, Sep.

2016.

[61] H. J. M. Hanley, W. M. Haynes, and R. D. McCarty, "The viscosity and thermal conductivity coefficients for dense gaseous and liquid methane," *J. Phys. Chem. Ref. Data*, vol. 6, no. 2, p. 597, Apr. 1977.

[62] A. Et-Tahir, C. Boned, B. Lagourette, and P. Xans, "Determination of the viscosity of various hydrocarbons and mixtures of hydrocarbons versus temperature and pressure," *Int. J. Thermophys.*, vol. 16, no. 6, pp. 1309–1334, Nov. 1995.

[63] H. J. M. Hanley and E. G. D. Cohen, "Analysis of the transport coefficients for simple dense fluids: The diffusion and bulk viscosity coefficients," *Phys. A Stat. Mech. its Appl.*, vol. 83, no. 2, pp. 215–232, Jan. 1976.

[64] K. C. Mo and K. E. Gubbins, "Conformal solution theory for viscosity and thermal conductivity of mixtures," *Mol. Phys.*, vol. 31, no. 3, pp. 825–847, Mar. 1976.

[65] K. C. Mo, K. E. Gubbins, G. Jacucci, and I. R. McDonald, "The radial distribution function in fluid mixtures: Conformal solution theory and molecular dynamics results," *Mol. Phys.*, vol. 27, no. 5, pp. 1173–1183, May 1974.

[66] J. F. Ely and H. J. M. Hanley, "Prediction of transport properties. 1. Viscosity of fluids and mixtures," *Ind. Eng. Chem. Fundam.*, vol. 20, no. 4, pp. 323–332, Nov. 1981.

[67] M. L. Huber, D. G. Friend, and J. F. Ely, "Prediction of the thermal conductivity of refrigerants and refrigerant mixtures," *Fluid Phase Equilib.*, vol. 80, pp. 249–261, Nov. 1992.

[68] B. a. Younglove and J. F. Ely, "Thermophysical Properties of Fluids. II. Methane, Ethane, Propane, Isobutane, and Normal Butane," *J. Phys. Chem. Ref. Data*, vol. 16. pp. 577–798, 1987.

[69] P. Ahmadi, A. Chapoy, and B. Tohidi, "Density, speed of sound and derived thermodynamic properties of a synthetic natural gas," *J. Nat. Gas Sci. Eng.*, vol. 40, pp. 249–266, Apr. 2017.

[70] A. Chapoy, R. Burgass, B. Tohidi, and I. Alsiyabi, "Hydrate and Phase Behavior Modeling in CO2-Rich Pipelines," *J. Chem. Eng. Data*, vol. 60, no. 2, pp. 447–453, Feb. 2015.

[71] A. G. Perez, A. Valtz, C. Coquelet, P. Paricaud, and A. Chapoy, "Experimental and modelling study of the densities of the hydrogen sulphide + methane mixtures at 253, 273 and 293 K and pressures up to 30 MPa," *Fluid Phase Equilib.*, vol. 427, pp. 371–383, 2016.

[72] L. M. C. Pereira, A. Chapoy, R. Burgass, and B. Tohidi, "Measurement and modelling

of high pressure density and interfacial tension of (gas+n-alkane) binary mixtures," *J. Chem. Thermodyn.*, vol. 97, pp. 55–69, 2016.

[73] M. H. Kapateh, A. Chapoy, R. Burgass, and B. Tohidi, "Experimental Measurement and Modeling of the Solubility of Methane in Methanol and Ethanol," *J. Chem. Eng. Data*, vol. 61, no. 1, pp. 666–673, Jan. 2016.

[74] M. Wise, A. Chapoy, and R. Burgass, "Solubility Measurement and Modeling of Methane in Methanol and Ethanol Aqueous Solutions," *J. Chem. Eng. Data*, vol. 61, no. 9, pp. 3200–3207, Sep. 2016.

[75] M. Wise and A. Chapoy, "Carbon dioxide solubility in Triethylene Glycol and aqueous solutions," *Fluid Phase Equilib.*, vol. 419, pp. 39–49, 2016.

[76] J. Kestin and W. Leidenfrost, "The effect of pressure on the viscosity of N2CO2 mixtures," *Physica*, vol. 25, no. 1–6, pp. 525–536, Jan. 1959.

[77] J. Kestin, Y. Kobayashi, and R. T. Wood, "The viscosity of four binary, gaseous mixtures at 20° and 30°C," *Physica*, vol. 32, no. 6, pp. 1065–1089, Jun. 1966.

[78] G. J. Gururaja, M. A. Tirunarayanan, and A. Ramachandran, "Dynamic viscosity of gas mixtures," *J. Chem. Eng. Data*, vol. 12, no. 4, pp. 562–567, Oct. 1967.

[79] J. Kestin, J. and Yata, "Viscosity and Diffusion Coefficient of Six Binary Mixtures," *J. Chem. Phys.*, vol. 49, no. 11, p. 4780, Sep. 1968.

[80] J. Kestin and S. T. Ro, "The Viscosity of Nine Binary and Two Ternary Mixtures of Gases at Low Density," *Berichte der Bunsengesellschaft für Phys. Chemie*, vol. 78, no. 1, pp. 20–24, Jan. 1974.

[81] J. Kestin, H. E. Khalifa, S. T. Ro, and W. A. Wakeham, "The viscosity and diffusion coefficients of eighteen binary gaseous systems," *Phys. A Stat. Mech. its Appl.*, vol. 88, no. 2, pp. 242–260, Aug. 1977.

[82] J. Kestin and S. T. Ro, "The Viscosity and Diffusion Coefficients of Binary Mixtures of Nitrous Oxide with Ar, N2, and CO2," *Berichte der Bunsengesellschaft für Phys. Chemie*, vol. 86, no. 10, pp. 948–950, Oct. 1982.

[83] J. Kestin, S. T. Ro, and W. A. Wakeham, "The transport properties of binary mixtures of hydrogen with CO, CO2 and CH4," *Phys. A Stat. Mech. its Appl.*, vol. 119, no. 3, pp. 615–638, May 1983.

[84] J. Kestin and S. T. Ro, "The Viscosity of Carbon-Monoxide Mixtures with Four Gases in the Temperature Range 25-200°C. Supplement," *Berichte der Bunsengesellschaft für Phys. Chemie*, vol. 87, no. 7, pp. 600–602, Jul. 1983.

[85] A. Hobley, G. P. Matthews, and A. Townsend, "The use of a novel capillary flow

viscometer for the study of the argon/carbon dioxide system," *Int. J. Thermophys.*, vol. 10, no. 6, pp. 1165–1179, Nov. 1989.

[86] V. A. Mal'tsev, O. A. Nerushev, S. A. Novopashin, V. V. Radchenko, W. R. Licht, E. J. Miller, and V. S. Parekh, "Viscosity of H2 −CO2 Mixtures at (500, 800, and 1100) K," *J. Chem. Eng. Data*, vol. 49, no. 3, pp. 684–687, May 2004.

[87] C. R. Locke, P. L. Stanwix, T. J. Hughes, M. L. Johns, A. R. H. Goodwin, K. N. Marsh, G. Galliero, and E. F. May, "Viscosity of {xCO2+(1−x)CH4} with x=0.5174 for temperatures between (229 and 348)K and pressures between (1 and 32)MPa," *J. Chem. Thermodyn.*, vol. 87, pp. 162–167, Aug. 2015.

Table 1. Available experimental viscosity data in the literature. *T*, temperature in K and *p*, pressure in MPa

Year	Phase	Mixture	*T*/K	*p*/MPa	No. of Exp. Point	Uncertainty	Ref.
1936	G	CO_2-O_2-CO-H_2- CH_4-N_2	293.15-1287		17	---	[53]
1959	G	CO_2-N_2	293.15	0.101-2.12	45	0.05%	[76]
1966	G	CO_2-N_2	293.15 &	0.101-2.53	12	0.10%	[77]
		CO_2-Ar	303.15				
1967	G	CO_2-O_2	295.15-303.15	0.098	7	---	[78]
		CO_2-N_2			6		
		CO_2-H_2			5		
		CO_2-O_2-H_2			12		
		CO_2-O_2-N_2			11		
1968	G	CO_2-CH_4	293.15 &	0.101-2.53	32	0.05%	[79]
		CO_2-Kr	303.15		24		
1974	G	CO_2-N_2	298.15-973.15	0.101	28	0.1- 0.3%	[80]
		CO_2-Ar			28		
		CO_2-He			56		
		CO_2-CH_4			20		
		CO_2-N_2-Ar			20		
		CO_2-N_2-CH_4			12		
1977	G	CO_2-O_2	298.15-674.15	0.101	15	0.1- 0.2%	[81]
1982	G	CO_2-N_2O	298.15-473.15	0.101	10	0.3%	[82]
1983	G	CO_2-H_2	295.15-303.15	0.101	3	0.10%	[83]
1983	G	CO_2-CO	298.15-473.15	0.101	10	0.10%	[84]
1989	G	CO_2-Ar	310.15-521.15	0.101	19	0.7%	[85]
2004	G	CO_2-H_2	500-800-1100	0.3	15	3%	[86]
2015	G-L	CO_2-CH_4	229 - 348	1 - 32	119	0.8%	[87]

Table 2. Compositions of the multi-component mixtures in mol% with the expanded uncertainties (coverage factor $k = 2$) in the parentheses

Components	CO_2 / mol%	MIX 1 / mol%	MIX 2 / mol%	MIX 3 / mol%
Carbon Dioxide	99.995	94.923	89.83	69.99
Methane	< 5 ppm	0.6261 (0.031)	0	20.02 (0.11)
Ethane	0	0	0	6.612 (0.034)
Propane	0	0	0	2.58 (0.013)
n-Butane	0	0	0	0.3997 (40 ppm)
i-Butane	0	0	0	0.3998 (40 ppm)
Nitrogen	< 25 ppm	1.41 (0.071)	5.05 (0.04)	0
Hydrogen	0	0.8175 (0.041)	0	0
Oxygen	< 10 ppm	0.8007 (0.004)	3.07 (0.10)	0
Argon		1.21 (0.061)	2.05 (0.06)	0
Carbon Monoxide	< 2 ppm	0.2127 (0.011)	0	0
Water	< 7 ppm	0	0	0
Total	100.00	100.00	100.00	100.00
Certification	Air Products	BOC	BOC	BOC
Analysis Method	SM [a]	SM [a]	SM [a]	SM [a]

[a] Supplier Method: The analysis techniques was based on the gas chromatography using flame ionization detector and thermal conductivity detector.

Table 3. Diameter calibration data using pure CO_2. T, temperature in K, p, pressure in MPa, D_{cal}, calibrated diameter in cm, η, viscosity in μPa.s, D_{old}, diameter before calibration in cm

					η / μPa.s			*AAD* / %	
No	Phase	*T*/K	*p*/MPa	D_{cal}/cm	$Exp_{D\text{-}old}$	REFPROP	$Exp_{D\text{-}cal}$	D_{old}	D_{cal}
1	Liq	238.2	10.22	0.02956	194.0	195.6	191.6	0.8	2.0
2	Liq	238.2	21.18	0.02956	212.0	214.7	209.4	1.2	2.4
3	Liq	238.2	51.70	0.02956	260.5	261.8	257.4	0.5	1.7
4	Liq	243.2	102.78	0.02956	320.4	313.7	316.3	2.2	0.8
5	Liq	243.2	126.15	0.02956	354.4	342.6	349.9	3.5	2.1
6	Liq	253.2	50.43	0.02955	218.2	216.9	215.0	0.6	0.9
7	Liq	253.2	102.56	0.02955	285.8	282.6	281.7	1.1	0.3
8	Liq	253.2	150.16	0.02955	348.7	337.7	343.8	3.3	1.8
9	Gas	273.2	1.05	0.02953	13.9	13.8	13.7	0.7	1.0
10	Gas	273.2	2.05	0.02953	14.1	14.1	13.9	0.5	1.2
11	Liq	273.2	10.47	0.02953	116.5	115.1	114.5	1.2	0.5
12	Liq	273.2	20.13	0.02953	134.0	132.0	131.7	1.5	0.2
13	Liq	273.2	52.05	0.02953	177.1	176.0	174.1	0.6	1.1
14	Liq	273.2	102.61	0.02953	234.5	234.0	230.5	0.2	1.5
15	Liq	273.2	150.44	0.02953	287.0	284.1	282.2	1.0	0.7
16	Gas	283.2	1.09	0.02952	14.6	14.3	14.3	2.1	0.2
17	Gas	283.2	2.07	0.02952	14.6	14.5	14.4	0.8	1.0
18	Liq	283.2	7.89	0.02952	93.1	92.5	91.4	0.7	1.2
19	Liq	283.2	23.07	0.02952	123.1	120.6	120.9	2.1	0.3
20	Liq	283.2	39.85	0.02952	146.5	143.9	143.8	1.8	0.1
21	Liq	283.2	59.01	0.02952	170.5	167.2	167.4	2.0	0.1
22	Liq	283.2	101.38	0.02952	216.6	213.2	212.7	1.6	0.2
23	Liq	283.2	151.26	0.02952	265.3	263.2	260.4	0.8	1.0
24	Gas	293.2	1.13	0.02951	14.9	14.8	14.6	0.7	1.3
25	Gas	293.2	2.05	0.02951	15.0	15.0	14.7	0.4	1.6
26	Liq	293.2	11.47	0.02951	88.3	85.4	86.5	3.3	1.3
27	Liq	293.2	20.37	0.02951	105.7	102.4	103.6	3.2	1.2
28	Liq	293.2	36.79	0.02951	132.0	125.9	129.5	4.9	2.8
29	Liq	293.2	68.99	0.02951	169.2	163.1	165.9	3.7	1.7
30	Liq	293.2	101.04	0.02951	199.2	196.0	195.3	1.6	0.3
31	Liq	293.2	141.60	0.02951	239.4	235.0	234.7	1.9	0.1
32	Gas	308.2	1.20	0.02949	15.7	15.5	15.3	0.9	1.3
33	Gas	308.2	2.07	0.02949	15.7	15.7	15.4	0.2	1.9
34	SC	308.2	11.33	0.02949	65.3	63.8	63.9	2.4	0.2
35	SC	308.2	22.09	0.02949	90.3	87.6	88.4	3.1	0.9
36	SC	308.2	34.97	0.02949	109.4	106.0	107.0	3.2	1.0
37	SC	308.2	68.93	0.02949	147.5	143.7	144.4	2.7	0.5
38	SC	308.2	101.20	0.02949	177.4	174.7	173.6	1.6	0.6
39	SC	308.2	150.52	0.02949	227.3	219.0	222.4	3.8	1.5
40	Gas	323.2	1.27	0.02948	16.5	16.3	16.1	1.6	0.7
41	Gas	323.2	2.05	0.02948	16.7	16.4	16.3	2.0	0.4
42	Gas	323.2	5.04	0.02948	17.8	17.4	17.4	2.2	0.2
43	SC	323.2	11.44	0.02948	40.7	41.2	39.8	1.1	3.4
44	SC	323.2	20.67	0.02948	72.8	70.5	71.1	3.3	0.8
45	SC	323.2	50.82	0.02948	114.7	109.9	111.9	4.4	1.9
46	SC	323.2	105.53	0.02948	164.5	160.8	160.6	2.3	0.1
47	SC	323.2	150.43	0.02948	200.0	198.6	195.3	0.7	1.6
48	Gas	373.2	1.48	0.02943	19.1	18.6	18.6	2.9	0.2
49	Gas	373.2	2.06	0.02943	19.3	18.7	18.7	3.3	0.2

					η / μPa.s			*AAD* / %	
No	Phase	*T*/K	*p*/MPa	D_{cal}/cm	$Exp_{D\text{-}old}$	REFPROP	$Exp_{D\text{-}cal}$	D_{old}	D_{cal}
50	Gas	373.2	5.15	0.02943	20.1	19.3	19.5	3.8	0.7
51	Gas	373.2	8.38	0.02943	21.6	20.8	21.0	4.1	1.0
52	SC	373.2	21.67	0.02943	41.5	41.0	40.2	1.2	1.8
53	SC	373.2	51.46	0.02943	80.7	78.0	78.3	3.4	0.3
54	SC	373.2	102.71	0.02943	122.9	117.8	119.2	4.3	1.2
55	SC	373.2	149.33	0.02943	154.8	149.9	150.1	3.2	0.1
56	Gas	423.2	1.71	0.02938	21.6	20.8	20.8	3.6	0.2
57	Gas	423.2	2.06	0.02938	21.6	20.9	20.8	3.6	0.2
58	Gas	423.2	5.13	0.02938	22.3	21.4	21.5	4.5	0.7
59	Gas	423.2	8.12	0.02938	23.1	22.2	22.3	4.3	0.4
60	SC	423.2	51.25	0.02938	61.7	60.6	59.4	1.9	1.8
61	SC	423.2	102.61	0.02938	98.6	94.5	95.0	4.4	0.5
62	SC	423.2	148.94	0.02938	125.6	121.0	121.0	3.8	0.0
Absolute Average Deviation (Total)								**2.2**	**1.0**

The standard uncertainties for the pressure and temperature measurements are:
$u(T)$ = 0.1 K and $u(p)$ = 0.02 MPa

Table 4. Validation data at two different isotherms using pure CO_2. T, temperature in K, p, pressure in MPa, η_{Exp}, experimental viscosity in μPa.s, $u_A(\eta)$ and $u_A(\eta)$, type A and B of uncertainty in viscosity in μPa.s, η_{Ref}, reference viscosity using Span-Wagner EoS in μPa.s

T = 308.2 K						T = 323.2 K					
p/MPa	η_{Exp}/μPa.s	$u_A(\eta)$/ μPa.s	$u_c(\eta)$/ μPa.s	η_{Ref}/μPa.s	$(\eta_{Exp}-\eta_{Ref})/\eta_{Exp}\times 100$	p/MPa	η_{Exp}/μPa.s	$u_A(\eta)$/ μPa.s	$u_c(\eta)$/ μPa.s	η_{Ref}/μPa.s	$(\eta_{Exp}-\eta_{Ref})/\eta_{Exp}\times 100$
This work											
1.20	15.3	0.0	0.2	15.5	-1.5	1.27	16.1	0.1	0.2	16.3	-0.7
2.07	15.4	0.0	0.2	15.7	-2.1	2.05	16.3	0.0	0.2	16.4	-0.4
11.33	63.8	0.1	0.2	63.3	0.8	5.04	17.4	0.1	0.2	17.4	0.0
22.09	88.2	0.4	0.4	87.1	1.2	11.44	39.8	0.2	0.3	40.1	-0.7
34.97	106.8	0.6	0.5	105.4	1.3	20.67	71.1	0.3	0.4	70.0	1.6
68.93	144.1	0.5	0.5	142.8	0.9	50.82	112.0	0.6	0.6	109.1	2.5
101.20	173.3	0.7	0.7	174.2	-0.5	105.53	160.6	0.3	0.8	159.6	0.6
150.52	222.0	0.3	0.8	217.3	2.1	150.43	195.3	0.4	0.9	196.9	-0.8
Al-Siyabi et al. [38] *											
8.31	42.4			42.4	0.1	8.95	23.1			23.0	0.6
10.79	61.3			61.2	0.2	12.23	45.3			45.1	0.4
13.68	70.5			70.3	0.2	17.25	62.9			62.7	0.3
17.57	79.2			79.1	0.2	22.35	73.2			73.0	0.2
24.06	90.5			90.3	0.3	27.60	81.6			81.4	0.3
26.86	94.6			94.4	0.2	31.72	87.3			87.1	0.3
33.07	103.4			102.9	0.4	35.56	92.3			92.0	0.4
42.67	115.2			114.7	0.4	39.17	96.8			96.3	0.5
45.15	118.6			117.6	0.9	47.45	106.3			105.6	0.7
Pensado et al. [39] **											
						15.00	58.3			56.5	3.0
						20.00	70.6			68.7	2.7
						25.00	79.6			77.4	2.7
						30.00	87.6			84.8	3.2
						35.00	92.8			91.3	1.6
						40.00	100.0			97.3	2.7
						45.00	106.0			102.9	2.9
						50.00	111.0			108.3	2.4
						55.00	117.0			113.4	3.0
						60.00	121.0			118.4	2.1

In this work, The standard uncertainties for the pressure and temperature measurements are:
$u(T)$ = 0.1 K and $u(p)$ = 0.02 MPa

* The uncertainties for the pressure, temperature and viscosity in Al-Siyabi et al. [38] were reported 0.02 MPa, 0.1 K and 1%, respectively.

** The uncertainties for the pressure, temperature and viscosity in Pensado et al. [39] were reported 0.1% of the full scale, 0.02 K and 3%, respectively.

Table 5. Parameters in the LBC and CO_2-LBC Viscosity Correlation

Parameters	LBC	CO_2-LBC
a_1	0.10230	0.10799
a_2	0.023364	0.035452
a_3	0.058533	0.021269
a_4	-0.040758	-0.013284
a_5	0.0093324	0.0034455

Table 6. Experimental results of the viscosity of MIX 1. T, temperature in K, p, pressure in MPa, η, experimental viscosity, $u_A(\eta)$, uncertainty type A, $u_c(\eta)$ uncertainty type B in µPa.s

No	Phase	T/K	p/MPa	η/µPa.s	$u_A(\eta)$/ µPa.s	$u_c(\eta)$/ µPa.s	No	Phase	T/K	p/MPa	η/µPa.s	$u_A(\eta)$/ µPa.s	$u_c(\eta)$/ µPa.s
1	Gas	243.2	1.48	12.7	0.1	0.2	32	Liq.	288.2	102.20	186.0	0.6	0.9
2	Liq.	243.2	21.11	168.6	1.2	0.8	33	Liq.	288.2	151.11	230.2	1.0	1.1
3	Liq.	243.2	52.54	217.3	1.0	1.0	34	Gas	298.2	2.08	15.3	0.0	0.2
4	Liq.	243.2	103.76	288.1	0.8	1.3	35	Gas	298.2	4.18	15.9	0.2	0.2
5	Liq.	243.2	151.14	349.8	1.4	1.6	36	Liq.	298.2	10.59	59.8	0.3	0.4
6	Gas	253.2	1.56	13.4	0.0	0.2	37	Liq.	298.2	20.66	81.0	0.5	0.4
7	Gas	253.2	2.04	13.4	0.1	0.2	38	Liq.	298.2	51.60	124.2	0.3	0.6
8	Liq.	253.2	21.53	144.0	0.8	0.7	39	Liq.	298.2	103.07	173.0	0.2	0.8
9	Liq.	253.2	52.04	193.9	0.8	0.9	40	Liq.	298.2	151.12	213.2	0.3	1.0
10	Liq.	253.2	103.74	260.2	0.9	1.2	41	SC	323.2	2.22	17.0	0.1	0.2
11	Liq.	253.2	151.65	314.4	0.4	1.5	42	SC	323.2	5.26	17.7	0.1	0.2
12	Gas	273.2	1.73	14.5	0.0	0.2	43	SC	323.2	6.97	18.7	0.1	0.2
13	Gas	273.2	2.11	14.6	0.1	0.2	44	SC	323.2	13.41	38.5	0.1	0.3
14	Gas	273.2	3.45	15.0	0.1	0.2	45	SC	323.2	20.45	60.3	0.3	0.4
15	Liq.	273.2	10.46	97.6	0.6	0.5	46	SC	323.2	51.13	100.5	0.3	0.5
16	Liq.	273.2	20.94	119.0	0.7	0.6	47	SC	323.2	103.26	145.2	0.8	0.7
17	Liq.	273.2	52.10	157.2	0.7	0.8	48	SC	323.2	151.25	180.8	0.5	0.9
18	Liq.	273.2	102.75	212.6	0.3	1.0	49	SC	373.2	2.66	19.3	0.0	0.2
19	Liq.	273.2	151.29	262.5	0.9	1.2	50	SC	373.2	5.22	19.9	0.1	0.2
20	Gas	283.2	1.81	14.9	0.1	0.2	51	SC	373.2	24.20	40.7	0.5	0.3
21	Gas	283.2	2.16	15.0	0.1	0.2	52	SC	373.2	52.04	72.6	0.1	0.4
22	Gas	283.2	3.49	15.5	0.1	0.2	53	SC	373.2	102.98	110.8	0.4	0.6
23	Liq.	283.2	10.41	78.5	0.7	0.4	54	SC	373.2	145.34	137.0	0.3	0.7
24	Liq.	283.2	21.08	104.4	0.9	0.5	55	SC	423.2	3.08	21.0	0.1	0.2
25	Liq.	283.2	51.67	145.1	0.7	0.7	56	SC	423.2	5.22	21.5	0.2	0.2
26	Liq.	283.2	103.18	196.7	0.8	0.9	57	SC	423.2	10.41	23.7	0.1	0.2
27	Liq.	283.2	151.00	242.0	0.4	1.1	58	SC	423.2	34.14	41.9	0.1	0.3
28	Liq.	288.2	9.02	67.8	0.7	0.4	59	SC	423.2	51.08	56.0	0.2	0.3
29	Liq.	288.2	16.58	88.7	0.2	0.5	60	SC	423.2	102.22	89.2	0.3	0.5
30	Liq.	288.2	34.23	115.6	0.3	0.6	61	SC	423.2	152.00	115.9	0.4	0.6
31	Liq.	288.2	48.29	132.6	0.6	0.7							

The standard uncertainties for the pressure and temperature measurements are $u(T)$ = 0.1 K and $u(p)$ = 0.02 MPa

Table 7. Experimental results of the viscosity of MIX 2. T, temperature in K, p, pressure in MPa, η, experimental viscosity, $u_A(\eta)$, uncertainty type A, $u_c(\eta)$ uncertainty type B in µPa.s

No	Phase	T/K	p/MPa	η/µPa.s	$u_A(\eta)$/ µPa.s	$u_c(\eta)$/ µPa.s	No	Phase	T/K	p/MPa	η/µPa.s	$u_A(\eta)$/ µPa.s	$u_c(\eta)$/ µPa.s
1	Liq.	243.2	21.40	162.2	1.5	0.8	24	Liq.	298.2	51.42	114.8	0.6	0.6
2	Liq.	243.2	51.95	207.5	1.4	1.0	25	Liq.	298.2	104.49	167.4	0.6	0.8
3	Liq.	243.2	103.29	260.8	2.2	1.2	26	Liq.	298.2	150.46	206.4	0.7	1.0
4	Liq.	243.2	151.69	329.8	2.4	1.5	27	Gas	323.2	2.57	16.7	0.2	0.2
5	Liq.	253.2	52.88	179.4	0.5	0.9	28	Gas	323.2	3.70	17.0	0.1	0.2
6	Liq.	253.2	104.06	239.0	1.7	1.1	29	SC	323.2	12.77	29.7	0.1	0.3
7	Liq.	253.2	152.66	289.3	1.7	1.4	30	SC	323.2	20.77	53.4	0.2	0.3
8	Gas	273.2	1.79	14.5	0.1	0.2	31	SC	323.2	52.43	95.2	0.2	0.5
9	Gas	273.2	2.26	14.0	0.2	0.2	32	SC	323.2	103.47	138.8	1.1	0.7
10	Liq.	273.2	21.08	107.0	0.9	0.5	33	SC	323.2	151.25	177.1	1.0	0.8
11	Liq.	273.2	52.31	142.9	0.9	0.7	34	Gas	373.2	1.53	18.8	0.2	0.2
12	Liq.	273.2	103.39	195.6	1.1	0.9	35	Gas	373.2	2.57	19.3	0.2	0.2
13	Liq.	273.2	151.09	241.7	1.3	1.1	36	SC	373.2	20.30	32.7	0.1	0.3
14	Gas	283.2	1.74	14.6	0.1	0.2	37	SC	373.2	51.86	68.3	0.2	0.4
15	Gas	283.2	2.28	14.7	0.2	0.2	38	SC	373.2	101.20	104.0	0.3	0.5
16	Liq.	283.2	20.28	89.4	0.6	0.5	39	SC	373.2	152.29	136.2	0.3	0.7
17	Liq.	283.2	52.66	125.0	1.0	0.6	40	Gas	423.2	2.42	20.9	0.2	0.2
18	Liq.	283.2	103.54	187.1	0.9	0.9	41	Gas	423.2	3.57	21.2	0.2	0.2
19	Liq.	283.2	151.55	230.8	0.4	1.1	42	SC	423.2	27.35	34.9	0.1	0.3
20	Gas	298.2	2.08	15.3	0.1	0.2	43	SC	423.2	51.81	54.1	0.1	0.3
21	Gas	298.2	3.53	15.2	0.2	0.2	44	SC	423.2	103.45	85.6	0.3	0.5
22	Liq.	298.2	10.42	43.1	0.2	0.3	45	SC	423.2	151.71	111.0	0.3	0.6
23	Liq.	298.2	20.57	73.8	0.4	0.4							

The standard uncertainties for the pressure and temperature measurements are $u(T)$ = 0.1 K and $u(p)$ = 0.02 MPa

Table 8. Experimental results of the viscosity of MIX 3. T, temperature in K, p, pressure in MPa, η, experimental viscosity, $u_A(\eta)$, uncertainty type A, $u_c(\eta)$ uncertainty type B in µPa.s

No	Phase	T/K	p/MPa	η/µPa.s	$u_A(\eta)$/ µPa.s	$u_c(\eta)$/ µPa.s	No	Phase	T/K	p/MPa	η/µPa.s	$u_A(\eta)$/ µPa.s	$u_c(\eta)$/ µPa.s
1	Gas	273.2	2.13	13.7	0.2	0.2	25	Gas	323.2	5.23	17.1	0.2	0.2
2	Liq.	273.2	12.92	64.5	0.4	0.4	26	SC	323.2	11.74	25.9	0.3	0.3
3	Liq.	273.2	20.94	76.8	0.7	0.4	27	SC	323.2	20.14	43.1	0.3	0.3
4	Liq.	273.2	52.31	109.7	0.5	0.6	28	SC	323.2	49.94	76.7	0.2	0.4
5	Liq.	273.2	104.24	156.9	1.0	0.8	29	SC	323.2	103.66	112.4	0.7	0.6
6	Liq.	273.2	124.73	167.6	0.5	0.8	30	SC	323.2	125.00	125.6	0.4	0.6
7	Liq.	273.2	152.00	188.3	0.9	0.9	31	Gas	373.2	2.15	18.5	0.2	0.2
8	Gas	283.2	2.09	13.7	0.1	0.2	32	Gas	373.2	5.24	19.2	0.2	0.2
9	Gas	283.2	4.89	18.0	0.2	0.2	33	Gas	373.2	10.44	20.7	0.1	0.2
10	Liq.	283.2	9.47	41.4	0.4	0.3	34	SC	373.2	20.72	31.8	0.2	0.3
11	Liq.	283.2	20.76	68.0	0.2	0.4	35	SC	373.2	46.22	56.4	0.4	0.3
12	Liq.	283.2	52.01	110.7	0.8	0.6	36	SC	373.2	63.26	67.3	0.1	0.4
13	Liq.	283.2	103.54	141.9	0.2	0.7	37	SC	373.2	103.20	87.8	0.3	0.5
14	Liq.	283.2	125.84	158.6	0.6	0.8	38	SC	373.2	125.26	102.4	0.2	0.5
15	Liq.	283.2	150.47	183.6	1.8	0.9	39	SC	373.2	151.47	119.1	1.1	0.6
16	Gas	298.2	1.11	13.5	0.1	0.2	40	Gas	423.2	5.22	20.7	0.1	0.2
17	Gas	298.2	2.09	14.9	0.2	0.2	41	Gas	423.2	10.36	22.1	0.1	0.2
18	Gas	298.2	5.18	15.8	0.1	0.2	42	Gas	423.2	20.96	26.7	0.2	0.3
19	SC	298.2	10.96	34.8	0.3	0.3	43	SC	423.2	29.11	34.7	0.2	0.3
20	SC	298.2	20.83	58.0	0.5	0.4	44	SC	423.2	49.79	48.4	0.2	0.3
21	SC	298.2	51.93	92.0	0.7	0.5	45	SC	423.2	102.95	75.1	0.3	0.4
22	SC	298.2	102.59	129.5	0.6	0.6	46	SC	423.2	124.68	84.6	0.3	0.4
23	SC	298.2	125.57	149.3	0.7	0.7	47	SC	423.2	146.38	94.4	0.6	0.5
24	Gas	323.2	2.11	16.6	0.1	0.2							

The standard uncertainties for the pressure and temperature measurements are $u(T)$ = 0.1 K and $u(p)$ = 0.02 MPa

Table 9. Average and maximum of estimated standard uncertainties of investigated mixtures

No	Material	Phase	No of exp. data	Estimated Standard Uncertainty Type A $u_A(\eta)$				Estimated Standard Uncertainty Type B $u_c(\eta)$			
				Average		Maximum		Average		Maximum	
				µPa.s	%	µPa.s	%	µPa.s	%	µPa.s	%
1	**MIX 1**	Gas	11	0.1	0.5	0.2	1.0	0.2	1.6	0.2	1.9
		Liquid	29	0.7	0.4	1.4	1.0	0.8	0.5	1.6	0.6
		SC	21	0.2	0.5	0.8	1.3	0.4	0.8	0.9	1.4
		Total	**61**	**0.4**	**0.5**	**1.4**	**1.3**	**0.6**	**0.8**	**1.6**	**1.9**
2	**MIX 2**	Gas	12	0.2	0.1	0.2	0.1	0.2	1.4	0.2	1.7
		Liquid	20	1.1	0.4	2.4	1.0	0.9	0.5	1.5	0.7
		SC	13	0.3	0.1	1.1	0.4	0.5	0.6	0.8	0.9
		Total	**45**	**0.6**	**0.2**	**2.4**	**1.0**	**0.6**	**0.8**	**1.5**	**1.7**
3	**MIX 3**	Gas	14	0.4	0.6	0.2	1.3	0.3	0.7	0.3	1.7
		Liquid	12	0.7	1.2	1.8	1.0	0.8	1.5	0.9	0.7
		SC	21	0.2	0.4	1.1	1.0	0.2	0.5	0.7	1.0
		Total	**47**	**0.4**	**0.6**	**1.8**	**1.3**	**0.4**	**0.8**	**0.9**	**1.7**
TOTAL		Gas	37	0.2	0.4	0.2	1.3	0.2	1.2	0.3	1.9
		Liquid	61	0.8	0.6	2.4	1.0	0.8	0.7	1.6	0.7
		SC	55	0.2	0.4	1.1	1.3	0.3	0.6	0.9	1.4
		Total	**153**	**0.5**	**0.4**	**2.4**	**1.3**	**0.5**	**0.8**	**1.6**	**1.9**

Table 10. Absolute average deviations between experimental viscosities and predictions of all fluids investigated in this work

1	2	3	4	5	6	7	8
No	Material	Phase	Data No	Absolute Average Deviation (AAD) / %			
				LBC	CO_2-LBC	LBC	CO_2-LBC
Density Correction?				Yes	Yes	No	No
1	**MIX 1**	Gas	11	6.2	16.4	6.2	16.5
		Liquid	29	4.9	3.1	25.4	20.7
		Supercritical	21	11.2	6.4	14.3	13.8
		Total	**61**	**7.3**	**6.7**	**18.1**	**17.6**
2	**MIX 2**	Gas	12	16.6	11.8	16.6	11.8
		Liquid	20	6.0	2.7	29.3	22.5
		Supercritical	13	8.6	3.7	12.5	14.8
		Total	**45**	**9.6**	**5.4**	**21.1**	**17.5**
3	**MIX 3**	Gas	14	14.6	11.1	14.6	11.1
		Liquid	12	21.0	24.0	46.0	42.2
		Supercritical	21	8.7	15.2	20.9	26.3
		Total	**47**	**13.6**	**16.2**	**25.4**	**25.9**
TOTAL		Gas	37	12.8	12.9	12.8	12.9
		Liquid	61	8.4	7.1	30.7	25.5
		Supercritical	55	9.6	9.1	16.4	18.8
		Total	**153**	**9.9**	**9.2**	**21.2**	**20.1**

Table 11. Absolute average deviations between experimental viscosities and predictions of all fluids investigated in this work

No	Material	Phase	Data No	Absolute Average Deviation (AAD) / %							
				ST	CO_2-ST	ST	CO_2-ST	CS2	CO_2-CS2	Ped	CO_2-Ped
Density Correction?				YES	YES	NO	NO	---	---	---	---
1	**MIX 1**	Gas	11	7.2	2.9	7.3	2.9	45.8	1.2	5.9	1.6
		Liquid	29	4.8	2.8	21.1	17.2	12.0	2.8	6.7	1.5
		SC	21	7.6	1.8	13.2	8.5	11.1	2.5	9.2	0.9
		Total	**61**	**6.2**	**2.5**	**15.9**	**11.6**	**17.8**	**2.4**	**7.4**	**1.3**
2	**MIX 2**	Gas	12	6.7	3.7	6.7	3.7	10.8	1.2	8.0	1.8
		Liquid	20	4.3	5.3	21.6	14.7	13.6	9.1	8.2	2.0
		SC	13	7.1	2.8	15.5	8.8	12.1	9.5	10.4	1.1
		Total	**45**	**5.7**	**4.1**	**15.9**	**10.1**	**12.4**	**7.1**	**8.8**	**1.7**
3	**MIX 3**	Gas	14	5.1	11.0	5.1	11.0	10.4	3.6	4.5	5.5
		Liquid	12	15.6	10.7	29.0	3.0	10.3	11.0	16.3	16.0
		SC	21	11.1	4.1	18.8	3.9	13.5	7.3	15.7	7.6
		Total	**47**	**10.5**	**7.8**	**17.3**	**5.8**	**11.8**	**7.2**	**12.5**	**9.1**
TOTAL		Gas	37	6.2	6.2	6.3	6.2	21.1	2.1	6.1	3.1
		Liquid	61	6.8	5.2	22.8	13.6	12.2	6.5	9.1	4.5
		SC	55	8.8	2.9	15.9	6.8	12.3	6.0	12.0	3.5
		Total	**153**	**7.4**	**4.6**	**16.3**	**9.4**	**14.4**	**5.3**	**9.4**	**3.8**

Table 12. Viscosity reduction of pure CO_2 in the presence of impurities for each system in the dense phase (Viscosity increases in the gas phase)

***T* / ºC**	***T* / K**	**Phase**	**Viscosity Reduction (%)**		
			MIX 1	**MIX 2**	**MIX 3**
0.0	273.15	Dense	11.2	18.1	38.5
10.0	283.15	Dense	11.5	17.8	38.0
25.0	298.15	Dense	13.0	21.4	37.8
25.0	298.15	Dense	10.6	19.8	32.6
100.0	373.15	Dense	6.5	10.8	21.4
150.0	423.15	Dense	4.5	7.8	17.3
		Impurity (%)	4.4	10.2	30.01
	Total	Gas	-0.9	-2.3	-8.9
		Dense	9.6	16.0	30.9

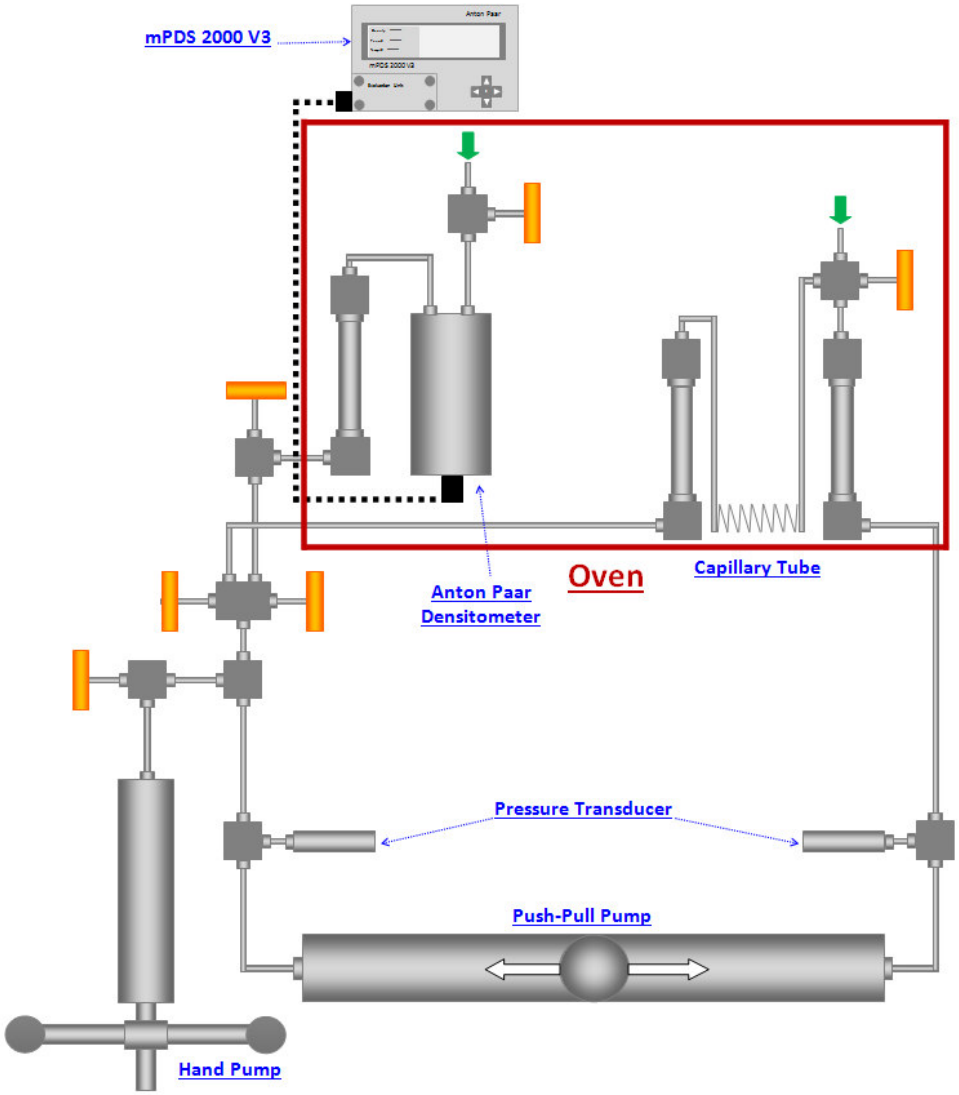

Figure 1. A schematic view of the viscosity experimental setup

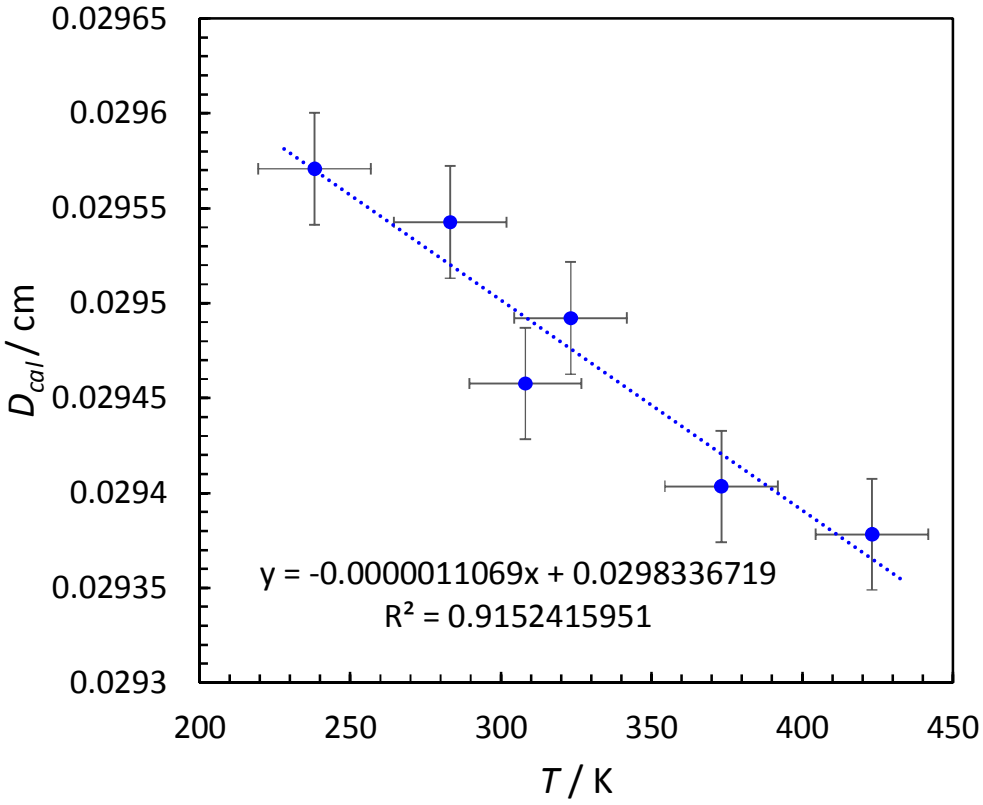

Figure 2. Calibrated diameter versus temperature

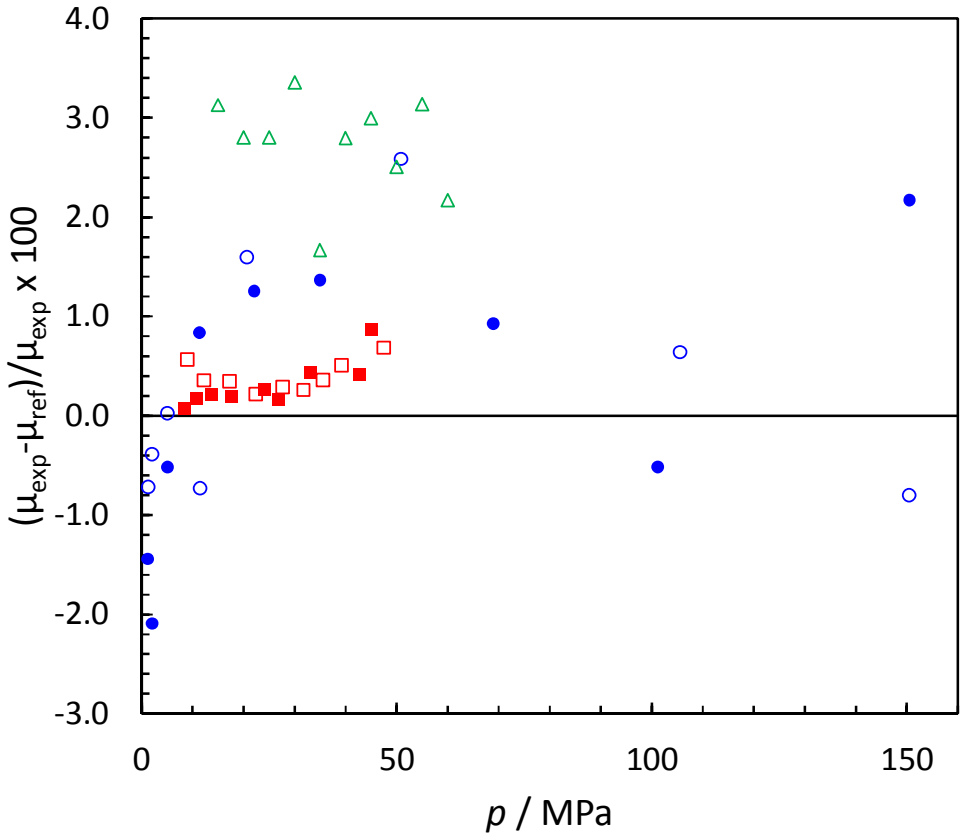

Figure 3. Deviations of pure CO_2 viscosity at different isotherms from predictions using CO_2-Pedersen, this work: (●) 308.2 K, (○) 323.2 K, Al-Siyabi et al., 2012 [38]: (■) 308.2 K, (□) 323.2 K, Pensado et al., 2008 [39]: (Δ) 323.2 K

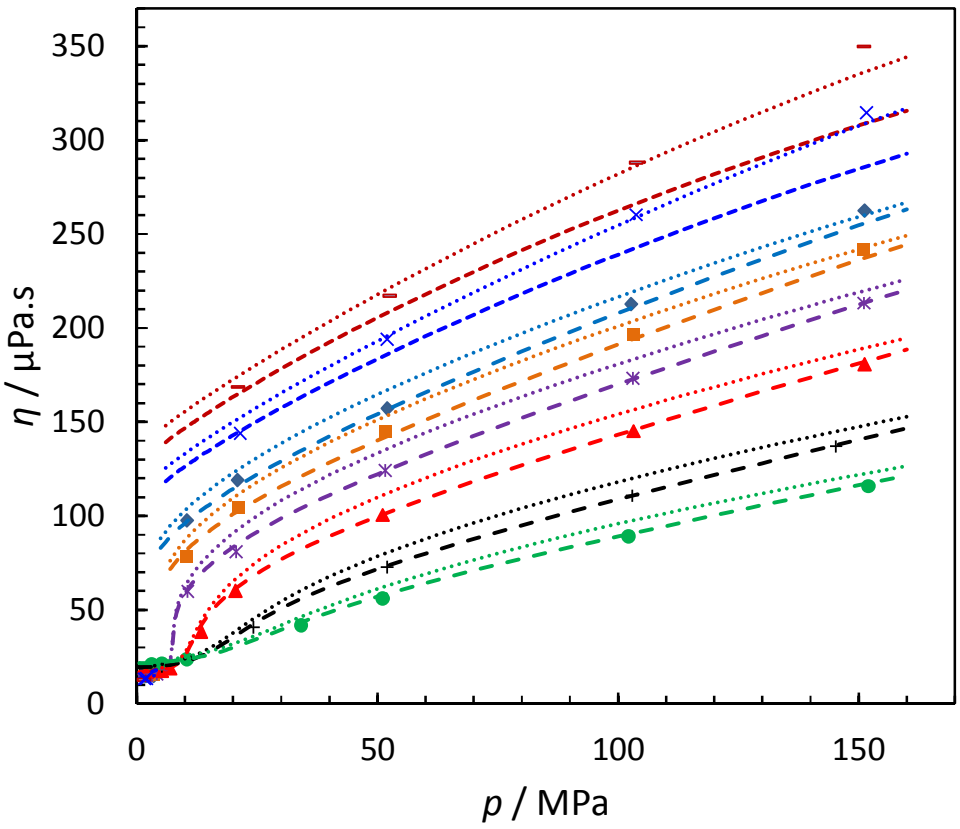

Figure 4. Experimental and modelling results (predictive models) of the viscosity of MIX 1 Experimental data: (-) at 243.2 K, (x) at 253.2 K, (♦) at 273.2 K, (■) at 283.2 K, (*) at 298.2 K, (▲) at 323.2 K, (+) at 373.2 K and (●) at 423.2 K, Modelling results: Round dot lines (…): Original SUPERTRAPP and dash lines (---) CO_2-SUPERTRAPP

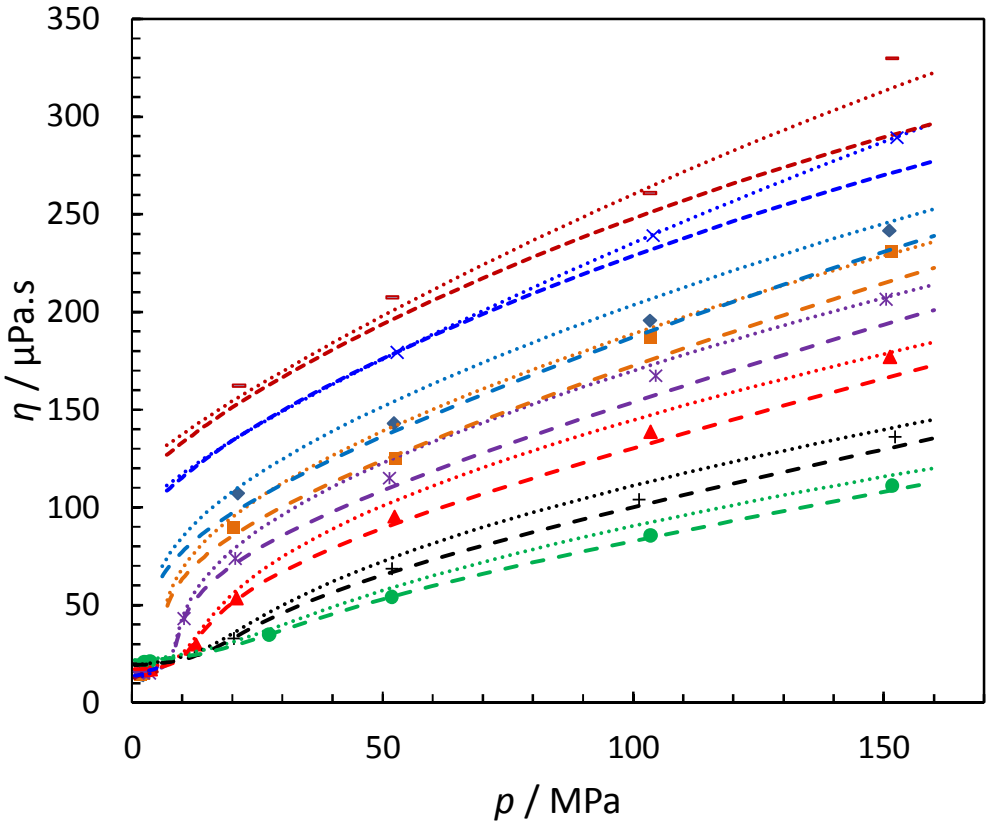

Figure 5. Experimental and modelling results (predictive models) of the viscosity of MIX 2 Experimental data: (-) at 243.2 K, (x) at 253.2 K, (♦) at 273.2 K, (■) at 283.2 K, (*) at 298.2 K, (▲) at 323.2 K, (+) at 373.2 K and (●) at 423.2 K, Modelling results: Round dot lines (…): Original SUPERTRAPP and dash lines (---) CO_2-SUPERTRAPP

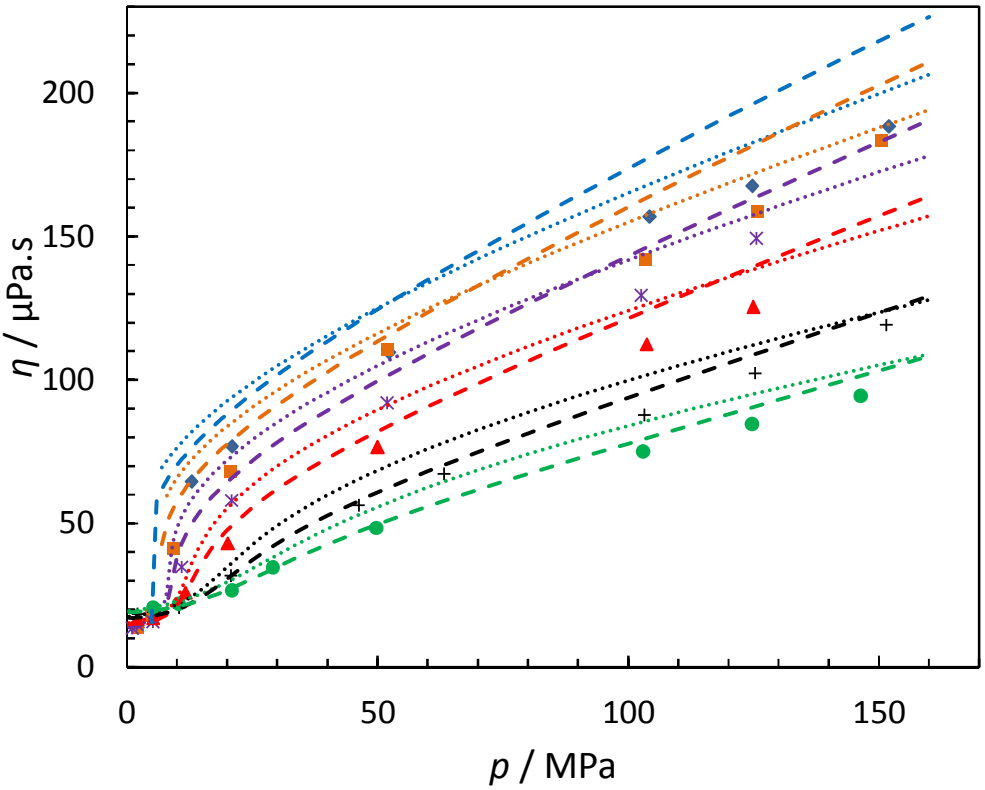

Figure 6. Experimental and modelling results (predictive models) of the viscosity of MIX 3 Experimental data: (♦) at 273.2 K, (■) at 283.2 K, (x) at 298.2 K, (▲) at 323.2 K, (+) at 373.2 K and (●) at 423.2 K, Modelling results: Round dot lines (…): Original Pedersen and dash lines (---) CO_2-Pedersen

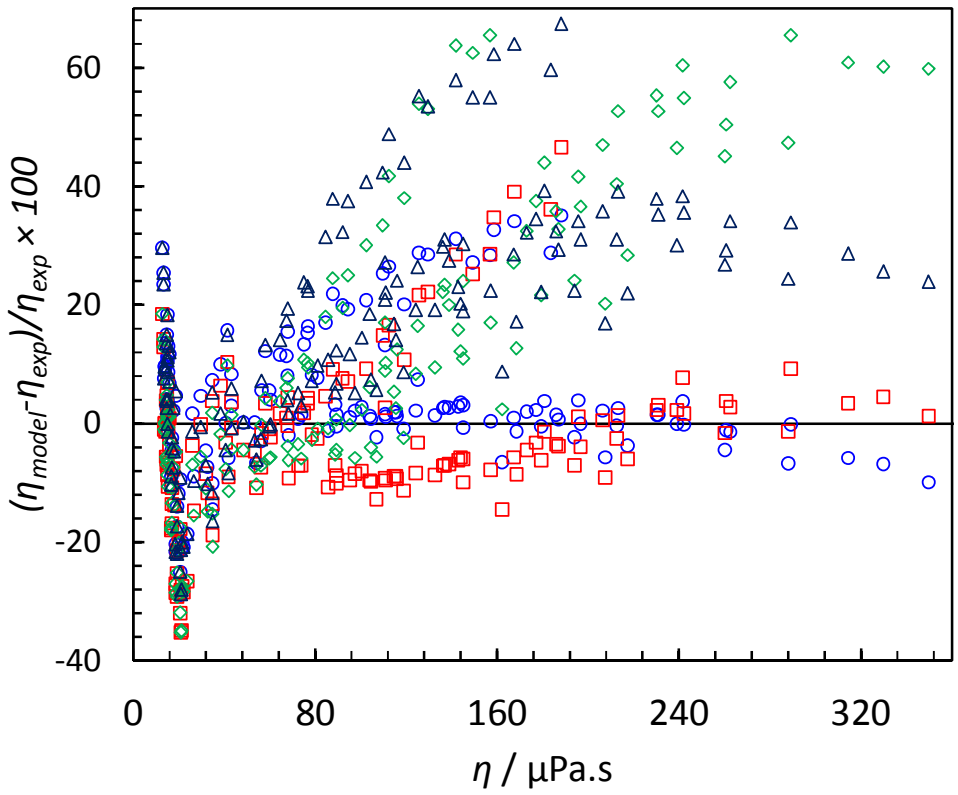

Figure 7. Deviations of LBC models from the experimental data to investigate the effects of tuning parameters and density correction, (○) CO_2-LBC &PR-CO_2, (□) LBC & PR-CO_2, (◊) LBC & PR, (Δ) CO_2-LBC & PR

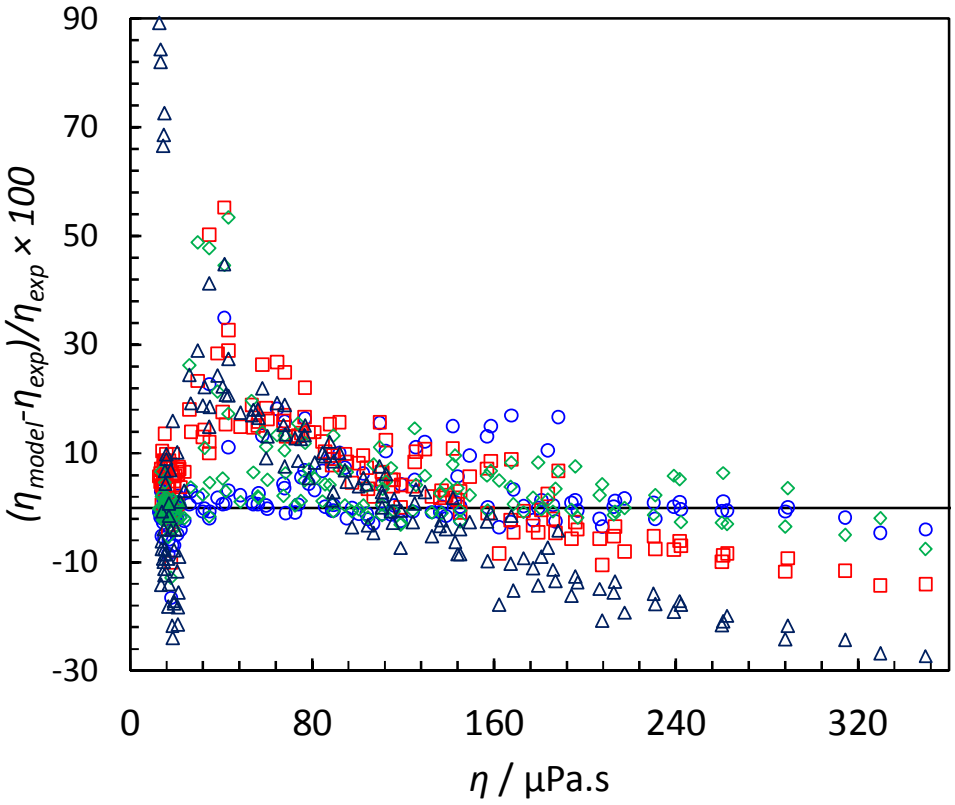

Figure 8. Deviations of predictive models from the experimental data, (○) CO_2-Ped, (□) Ped, (◊) CO_2-CS2 (Δ) CS2

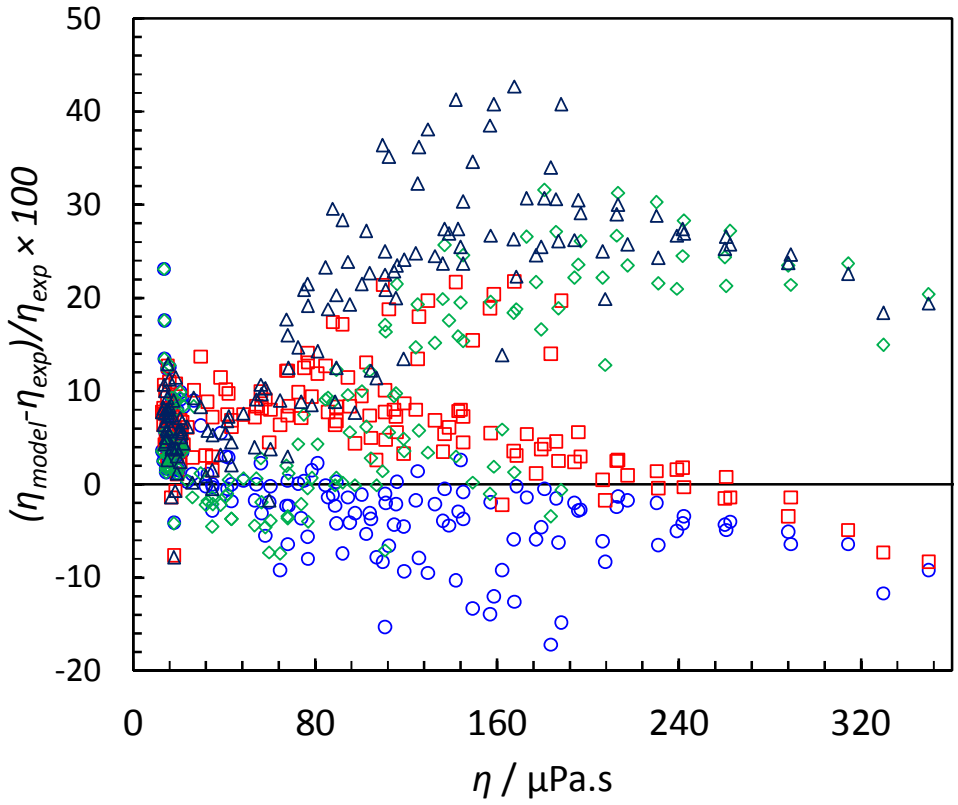

Figure 9. Deviations of SUPERTRAPP models from the experimental data to investigate the effects of modification and density correction, (○) CO_2-ST &PR-CO_2, (□) ST & PR-CO_2, (◊) CO_2-ST & PR, (Δ) ST & PR

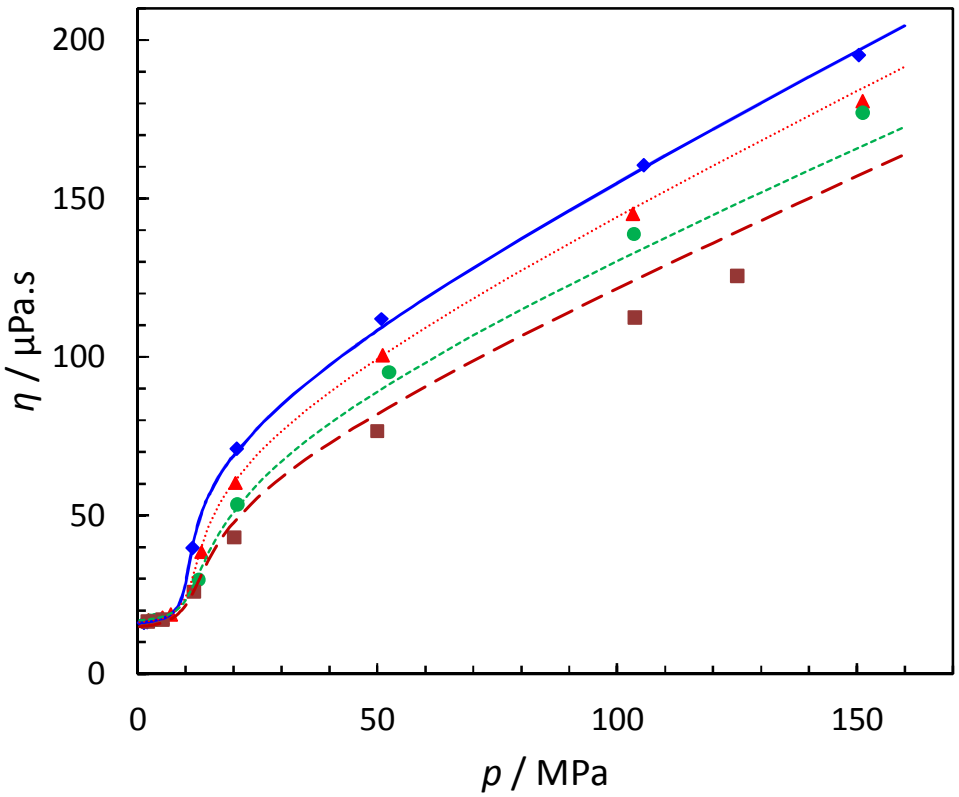

Figure 10. The effect of impurities on viscosity of pure CO_2 at 323.2 K, experimental data / modelling using CO_2-Pedersen: (♦/___) Pure CO_2, (▲/….) MIX 1, (●/----) MIX 2, (■/_ _ _) MIX 3

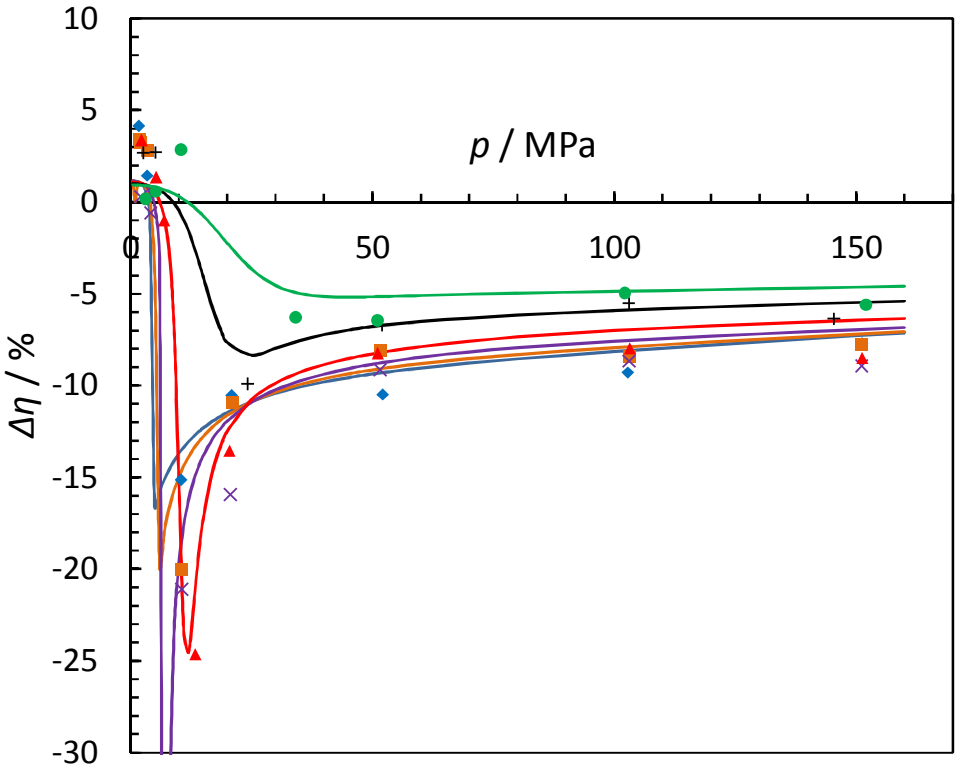

Figure 11. The viscosity changes from pure CO_2 for MIX 1 at different temperatures. Experimental data: (♦) at 273.2 K, (■) at 283.2 K, (x) at 298.2 K, (▲) at 323.2 K, (+) at 373.2 K and (●) at 423.2 K, Modelling results: lines (—) CO_2-Pedersen

Highlights:

- Viscosities of three multi component CO_2-rich mixtures were measured.
- New experimental data were reported in the gas, liquid and supercritical phases.
- Pedersen and SUPERTRAPP models were modified for systems contain high CO_2.
- The effect of density corrections on the viscosity predictions were investigated.
- The measured viscosity data were employed to evaluate various modified models.